CENTRAL RESEARCH LIBRARY

ORNL-TM-3850

LOCKHEED MARTIN ENERGY RESEARCH LIBRARIES

3 4456 0514763 1

NEUTRON-INDUCED GAMMA-RAY PRODUCTION IN IRON FOR THE ENERGY RANGE $0.8 \leq E_n \leq 20$ MeV

J. K. Dickens
G. L. Morgan
F. G. Perey

OAK RIDGE NATIONAL LABORATORY
CENTRAL RESEARCH LIBRARY
DOCUMENT COLLECTION
LIBRARY LOAN COPY
DO NOT TRANSFER TO ANOTHER PERSON
If you wish someone else to see this document, send in name with document and the library will arrange a loan.
UCN-7969
(3 3-67)

OAK RIDGE NATIONAL LABORATORY
OPERATED BY UNION CARBIDE CORPORATION • FOR THE U.S. ATOMIC ENERGY COMMISSION

This report was prepared as an account of work sponsored by the United States Government. Neither the United States nor the United States Atomic Energy Commission, nor any of their employees, nor any of their contractors, subcontractors, or their employees, makes any warranty, express or implied, or assumes any legal liability or responsibility for the accuracy, completeness or usefulness of any information, apparatus, product or process disclosed, or represents that its use would not infringe privately owned rights.

LOCKHEED MARTIN ENERGY RESEARCH LIBRARIES

3 4456 0514763 1

ORNL-TM-3850

Contract No. W-7405-eng-26

Neutron Physics Division

NEUTRON-INDUCED GAMMA-RAY PRODUCTION IN IRON FOR THE ENERGY RANGE $0.8 \leq E_n \leq 20$ MeV

J. K. Dickens, G. L. Morgan and F. G. Perey

AUGUST 1972

NOTE: THIS WORK FUNDED BY DEFENSE NUCLEAR AGENCY UNDER SUBTASK No. PC101

OAK RIDGE NATIONAL LABORATORY
Oak Ridge, Tennessee 37830
operated by
UNION CARBIDE CORPORATION
for the
U. S. ATOMIC ENERGY COMMISSION

CONTENTS

Page No.

I. Introduction 1

II. Experimental Methods and Data Reduction 3

A. NaI Experiment 3

B. Ge(Li) Experiment 21

C. Experimental Results for n + ^{54}Fe 25

D. Excitation of the 846-keV Level in ^{56}Fe Near Threshold . . . 28

III. Discussion and Comparison of Data 29

A. Comparison of E_γ = 846-keV Data 29

B. Comparison of E_γ = 1.24-MeV Data 35

C. Discussion of Remaining Gamma-Ray Data 37

IV. Summary and Conclusions 46

V. Acknowledgements 47

APPENDIX 52

ABSTRACT

Cross sections for production of gamma rays due to neutron interactions with iron have been measured as a function of both neutron and gamma-ray energy. Two experimental configurations were used to obtain the data, and these were (a) a NaI-spectrometer system using the Oak Ridge Linear Accelerator as the neutron source, and (b) a Ge(Li)-spectrometer system using a pulsed Van de Graaff and the D(d,n) reaction as the neutron source. The NaI-spectrometer system is described completely in this report. It was used to acquire data for $0.8 \leq E_n \leq 20$ MeV and $\theta_\gamma = 125$ deg, which were unfolded to obtain $d^2\sigma/d\omega dE$ values for gamma-ray energies between 0.7 and 10 MeV. The Ge(Li) system was used to obtain high-resolution information on the production of discrete-line $d\sigma/d\omega$ values for $4.85 \leq E_n \leq 9.0$ MeV and $\theta_\gamma = 55$, 75 and 90 deg. Our data are compared with previously reported experimental data and with the current ENDF/B evaluation. Although there is generally reasonable (20%) agreement, important differences among these data are discussed.

I. INTRODUCTION

There are many applications, for example to compute the efficacy of neutron shields, for which neutron-induced gamma-ray production cross sections are required. As a result, many requests for such cross sections have been tabulated.[1] This paper reports measurements for the production cross sections for gamma radiation resulting from neutron interactions with Fe for incident neutron energies between 0.86 MeV (threshold for inelastic scattering from ^{56}Fe) and 20 MeV. For this range of neutron energies, many groups have reported gamma-ray production cross sections. The more recent reports include Benjamin *et al.*,[2] Texas Nuclear (TNC) for E_n between 0.95 and 4.0; Drake *et al.*,[3] Los Alamos Scientific Laboratory (LASL) from E_n between 4.0 and 7.67 MeV; Broder *et al.*,[4] Obninsk for E_n between 0.93 and 7.37 MeV; Haouat *et al.*,[5] Commissariat a l'Energie Atomique (CEA) for E_n between 2.5 and 8.8 MeV; and Orphan *et al.*,[6] Gulf Radiation Technology (GRT) for E_n between 0.86 and 16.74 MeV. However, these reports do not always agree well among themselves nor with earlier work,[7] and in several cases the uncertainties assigned to absolute cross sections are rather large (20% or more). One result of the experimental disagreements and uncertainties has been the difficulty in creating a satisfactory gamma-ray file for the ENDF evaluation for Fe, especially for $E_n > 4$ MeV. The present study was undertaken to obtain a complete and consistent data set with smaller uncertainties which would lead to a better understanding of the distribution of absorbed neutron flux by Fe.

The most recent experiments[4-6] employed Ge(Li) detectors and revealed (especially in the CEA report[5]) a wealth of information about discrete gamma rays. Correlating the gamma rays observed with particular transitions

between levels of ^{56}Fe, excited by inelastic scattering, has proved difficult especially for levels above an excitation energy of 4 MeV. The best experimental information concerning deexcitation of highly excited states in ^{56}Fe has come from the study of ^{56}Co beta decay.[8,9] We have obtained a number of spectra using a good-resolution Ge(Li) detector system with emphasis on obtaining branching-ratio information as well as production cross sections as a function of E_n and θ_γ for individual gamma-ray transitions in ^{56}Fe. Spectra which were obtained for $E_n > 9$ MeV proved unsatisfactory for both objectives. We did not observe new high-energy transitions in these spectra, suggesting that either highly excited states decay by cascade transitions to intermediate energy levels or there are many very weak transitions and our energy resolution was inadequate to resolve them. Even with the presently available good-resolution Ge(Li) spectrometer, such radiation will appear as a "continuum".[10] This observation verifies that of GRT;[6] for $E_n >$ 7.7 MeV these authors report < 45% of the total gamma-ray production cross section in discrete lines with the remainder reported as a "continuum".

For many applications, the detailed information on deexcitation of many individual states is not required, and may not even be desired, in view of the data handling problems. In order to satisfy the needs for complete and consistent gamma-ray information in applications such as shielding, we have set up a facility to measure neutron gamma-ray production data at the Oak Ridge Electron Linear Accelerator (ORELA) Shield Test Station. A NaI-detector spectrometer system is used with ORELA as the neutron source. The system was first used to study gamma-ray

production cross sections for samples of tantalum and carbon.[11] We have used this system to obtain similar data for iron samples for neutron energies between 0.86 and 20 MeV.

The scope of this report is as follows. In Section II the experimental system is presented, with particular emphasis on the NaI spectrometer. In addition we present some of the Ge(Li) data for samples of both ^{nat}Fe and ^{54}Fe (isotopic abundance 5.8%). We also demonstrate the capabilities of our system for measuring high neutron-energy resolution cross sections for the first excited state in ^{56}Fe. Section III is devoted to comparing the present data with some of the recently published work[2-6,12] and with the gamma-ray file of the most recent evaluation[13] (ENDF/B Mat 4180). However, unlike our previous reports[14,15] of gamma-ray production cross sections for other elements, we do not present a detailed analysis of the data. The quantity and diversity of the data for n + Fe requires considerable study to arrive at a consistent overall set of cross sections - a task beyond this report.

II. EXPERIMENTAL METHODS AND DATA REDUCTION

A. NaI Experiment

A general schematic of the experimental layout is shown in Figure 1. The ORELA was used to provide the electron beam. Neutrons were produced by photonuclear processes due to bremstrahlung from electron impact on a tantalum target.[16] For this experiment the electron energy was about 130 MeV with a repetition rate of 800 pulses per second. For most of the data reported here, except where specifically indicated, a pulse width of 10 nsec with a total electron beam power of 12 kW was used.

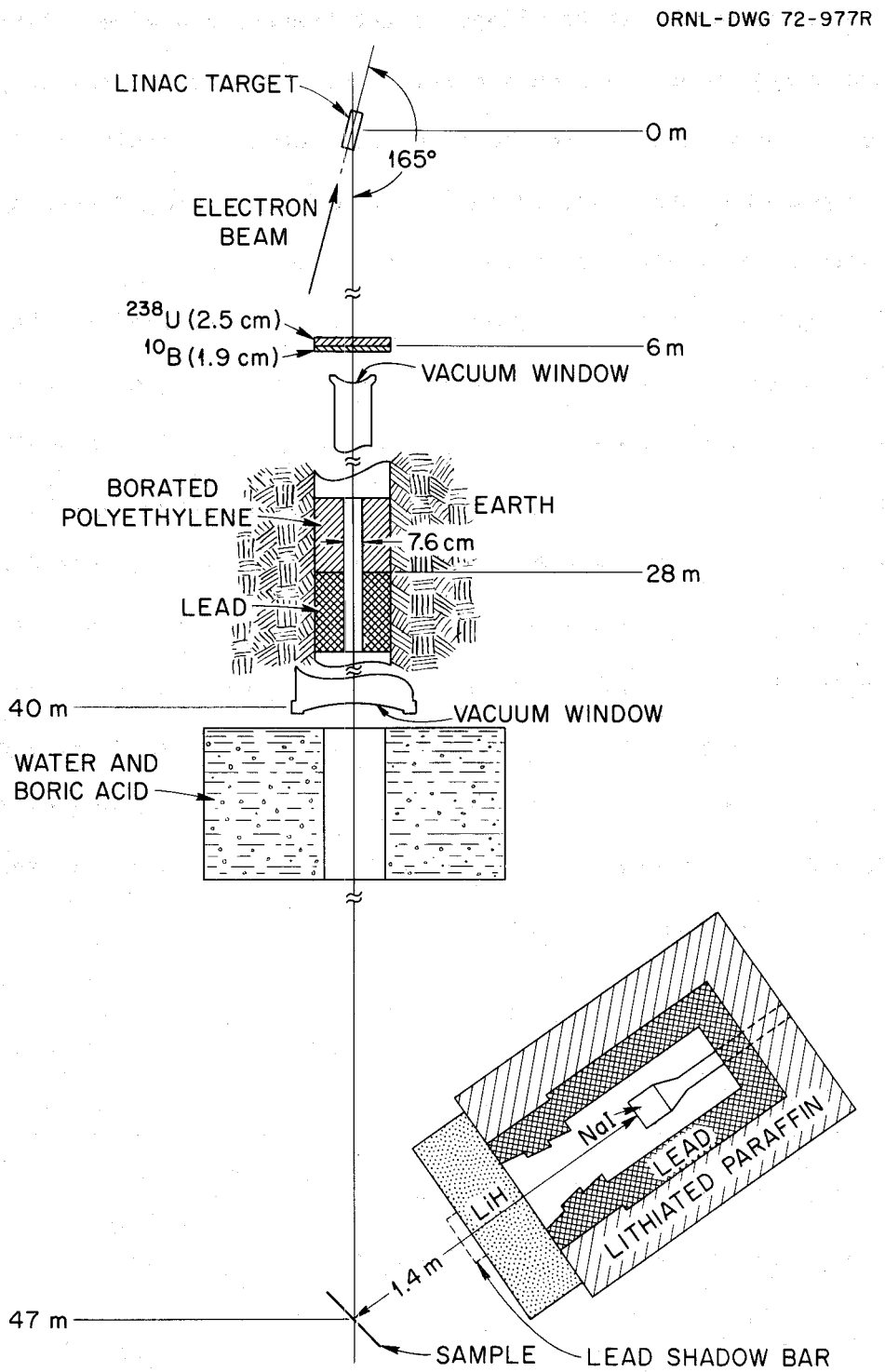

Fig. 1. Experimental arrangement showing neutron source, flight path with collimators and filters, and NaI spectrometer. The shadow bar shown dotted is used for background measurements.

Neutrons produced at the linac target traversed a 47-m flight path and were incident on the iron sample. About 40 m of the flight path was under vacuum in order to increase the neutron intensity at 47 m and to reduce the structure in the neutron flux due to scattering resonances in air. The neutron beam was stopped in a concrete catcher located about 5 m behind the sample. Gamma rays produced in the sample were observed by a 12.7 x 12.7 cm NaI crystal located inside a substantial shield made of lead and "lithiated paraffin". (The "lithiated paraffin" bricks were made by incorporating lithium carbonate into the paraffin when the bricks were cast.) The NaI detector was shielded against neutrons scattered from the sample by a 25-cm-thick, 1-m-diam slab of lithium hydride placed in front of the collimator.

The iron sample consisted of a 30 x 30 x 0.64 cm slab. The density of the iron was 7.87 g/cm^3. The sample was analyzed for impurities which were found to be present in amounts smaller than 0.03% except Mn (0.77%), C (0.21%), Mo (0.07%) and Ni (0.07%).

A filter consisting of 1.9 cm of ^{10}B was located in the neutron beam 5 m from the linac target. This filter removed "all" neutrons of less than 1 keV energy, preventing overlap between neutrons of adjacent accelerator pulses. Also located at 5 m was a 2.5-cm-thick filter of depleted uranium to reduce the intensity of the gamma flash at 47 m. The diameter of the neutron beam at the sample position was limited to 15 cm by a 7.6-cm-diameter collimator located 28 m from the linac target (see Figure 1). Careful measurements were made of the profile of the neutron beam at the sample position, 47 m, using a 6 x 6 mm plastic scintillator; one such profile in the horizontal plane is shown in the inset of Figure 2. From

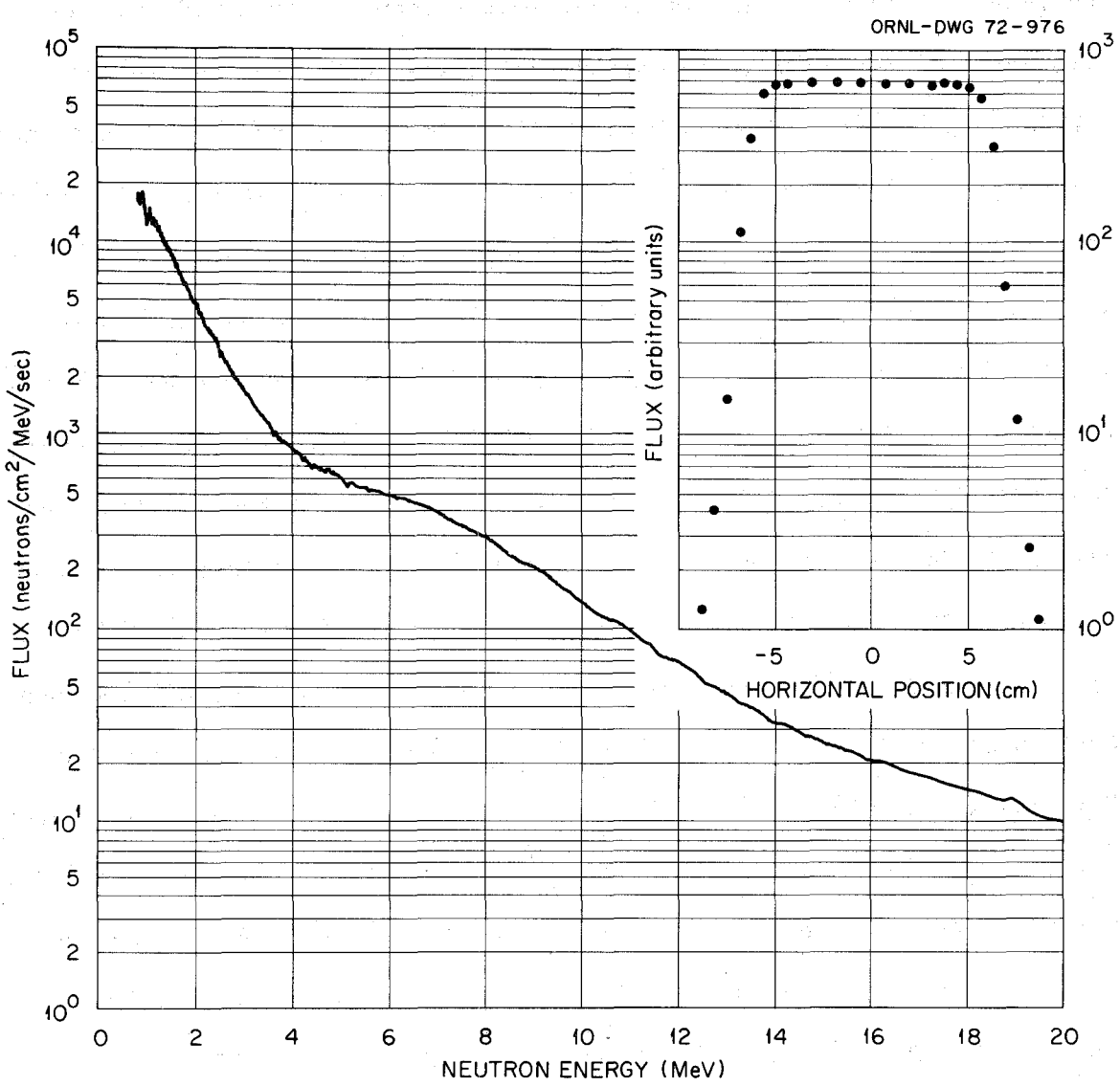

Fig. 2. Measured neutron flux at 47.35 m for beam power 21 kW. The inset shows the profile of the neutron beam at the sample position.

the profile measurements we can determine the effective neutron beam area at the sample, a quantity required to relate counting rates to cross sections. In view of the simple collimator geometry employed, we can also use the profile measurements to calculate an "effective neutron source area" at the linac target. The profile measurements indicate that the neutron source, at the linac target, has linear dimensions of approximately 2.5 cm. From this dimension, of the order of the size of the tantalum target,[16] we deduce that most of the neutrons reaching the sample, in the MeV region, emanate from the tantalum target rather than from its water cooling jacket. We are therefore confident that the neutron energy spectrum shape measured along the axis of the neutron beam applies reasonably well to the complete beam area. A direct check on this was made by comparing the flux shapes obtained by time of flight with a 5 x 5 cm NE-213 detector placed (a) along the beam axis and (b) 5 cm off the beam axis. The two measurements gave neutron energy spectral shapes which agree to better than $\pm 3\%$ over the complete energy range from 1 to 20 MeV. A second determination of the effective neutron beam area was made by comparing the neutron induced gamma-ray counting rate from the sample used in the experiment, which covered the whole neutron beam, to that obtained from a small (4 x 4 cm) iron slab of identical thickness and composition located at the center of the beam. Measurements using the two approaches were in agreement to within 5%.

The neutron flux was measured along the neutron beam axis at the sample position by time-of-flight using a 5 x 5 cm NE-213 scintillator counter. The integral neutron efficiency of the detector as a function of energy was obtained from Verbinski *et al.*[17] who used a detector with the same

diameter. The result of this measurement, normalized to 21 kW of electron beam power, is shown in Figure 2. For the flux measurement the same filters were in the flight path, and ORELA was operated at the same electron energy (130 MeV) but with the short pulses (≈5 nsec) and very low beam power (< 1 kW). A neutron monitor counter[18] located in the linac target vault was used to normalize the flux to the accelerator conditions used in the gamma-ray measurements. A second neutron flux monitor was used in the experiment, a 6 x 6 mm plastic scintillator located in the edge of the neutron beam after the collimator at the 28 m station of the flight path. During all runs a time-of-flight spectrum was recorded from this plastic scintillator. Numerous checks have been made of the consistency of these two independent monitors as a function of electron energy, beam power and pulse width. From these measurements we have concluded that both the relative shape of the neutron energy spectrum from 1 to 20 MeV and the absolute normalization of this spectrum are determined to within 10% for the conditions prevailing during the gamma-ray production measurements. These flux measurements, together with the neutron beam area determinations described earlier, were used to determine the number of neutrons per unit energy incident on the sample.

A diagram of the electronics used for the gamma-ray measurement is shown in Figure 3. The anode of a phototube on the NaI crystal provided a fast signal which passed through a timing-filter amplifier and a constant-fraction discriminator. This output served as the stop signal for a time-to-amplitude converter which was started by a fiducial signal based on the linac gamma flash. The fiducial signal is obtained from a

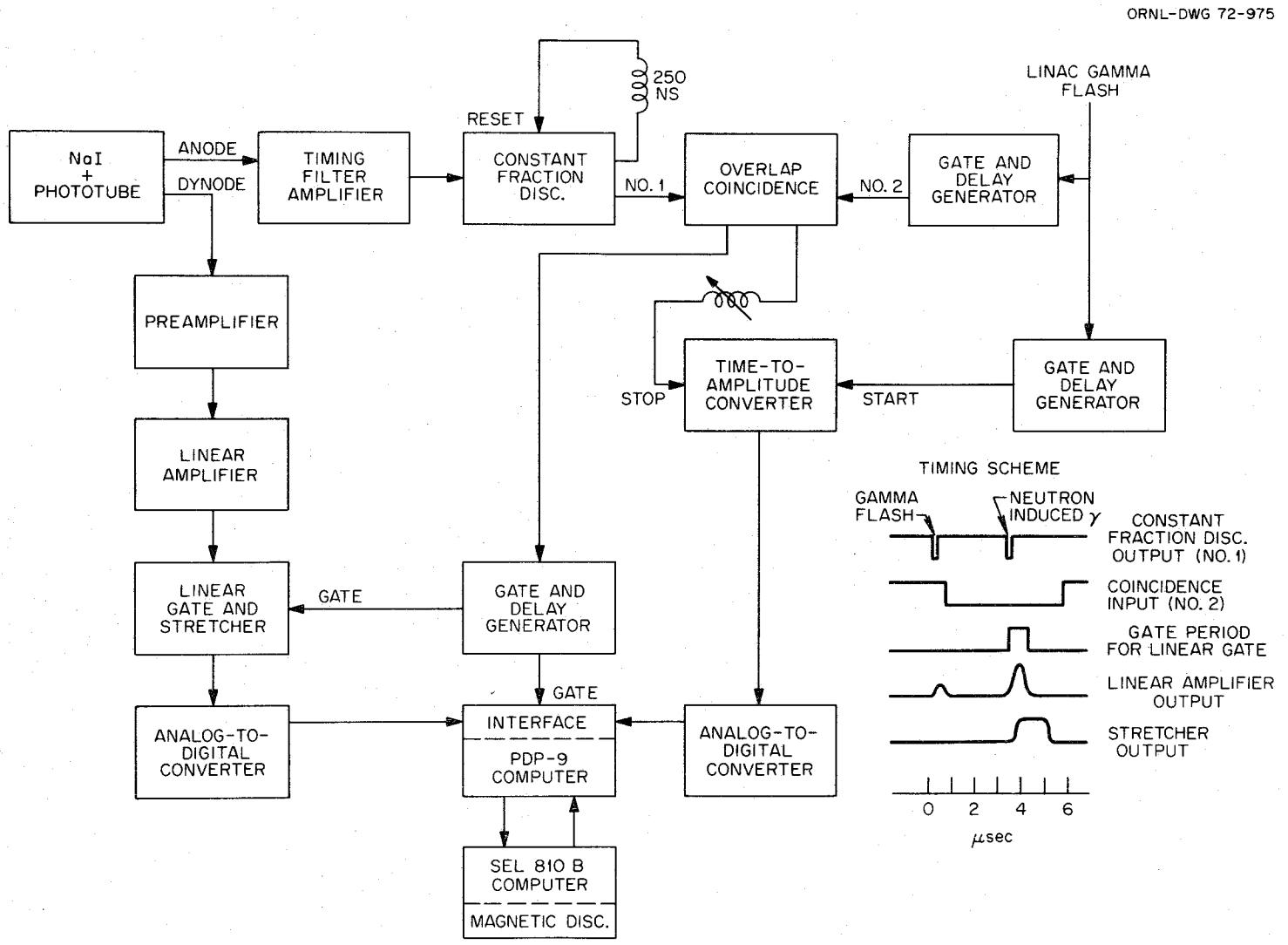

Fig. 3. Block diagram of the electronics used for the gamma-ray measurements.

bare phototube which views the linac target directly. The time resolution of the crystal and electronics system was < 5 nsec. Coincidence gating was used to exclude the gamma flash scattered by the sample. Because of the uranium filter, the gamma flash seen by the spectrometer was quite small (only 20% of the linac pulses produced gamma-flash events in the NaI greater than 500 keV). A clipping time of 100 nsec in the main amplifier, used in conjunction with a linear gate and stretcher, insured that the gamma flash signal did not interfere with signals due to neutron-induced gamma rays from the sample for all $E_n \leq 20$ MeV. The time-of-flight (TOF) and pulse-height (PH) signals were digitized and presented to a PDP-9 computer which correlated the events and sent the TOF-PH pairs to the ORELA-SEL-810B computer for storage on magnetic discs in a 512 x 512 channel array (see Ref. 19 for a description of this data acquisition system). In addition, a 2048-channel spectrum of time-of-flight for all pulse heights greater than the fast discriminator level was stored on disc. A 512-channel spectrum of pulse height for all time-of-flight within the coincidence period was also stored. The data accumulated on disc were written on magnetic tape to be reduced later on an IBM 360 system.

The response of the spectrometer must be known to unfold the pulse-height distributions to obtain gamma-ray energy spectra. For the spectrometer used in the present work, response functions were measured over the gamma-ray energy range from 0.66 to 6.13 MeV using a series of calibrated sources located at the sample position. The measured responses thus included all the characteristics of the spectrometer. That is - in addition to the intrinsic response of the crystal itself - the effective

solid angle, the gamma-ray attenuation and inscattering in the LiH shield, and the effects of scattering in the lead collimator and shield were all included in the response function measurements. Measurements were taken for sources in the front and the back of the iron sample; the effect of scattering of the gamma rays by the sample could not be detected in the response function shape. Sources used in these measurements included ^{137}Cs, ^{54}Mn, ^{22}Na, $H(n,\gamma)$, ^{24}Na, ^{241}Am-Be and ^{244}Cm-^{13}C (for E_γ = 6.13 MeV (Ref. 20)). For E_γ > 6.13 MeV responses measured at the ORNL Tower Shielding Facility[21] using a crystal of identical size were employed after taking into account the solid angle and LiH transmission as calculated from the dimensions of the spectrometer. Using all of these response functions, a response matrix was generated by an interpolation procedure. The method of interpolation was similar to the one employed for generating the response matrix for the ORNL Tower Shielding spectrometer.[21] The response matrix was square using 125 bins to cover the gamma-ray energy and pulse-height ranges from 0.69 to 10.6 MeV. The bin widths were chosen so as to give about 2 to 3 bins per resolution width of the detector. Because of the short clipping time and the LiH shield, the energy resolution of our NaI detector was not optimal and varied from about 10% at 1 MeV to 5% at 6 MeV.

To test the response functions thus obtained, as well as the computer routines used in the unfolding, a spectrum of a known ^{226}Ra source was obtained. This source has 48 (or more) discrete gamma rays for E_γ between 0.7 and 3.0 MeV having well-measured intensities.[22,23] The relative intensities of the strongest lines have been determined to within a few percent accuracy. The unfolding code used was FERD (see Refs. 24-26

for a description of this code and its application to unfolding of NaI spectra). The window functions used for each bin was a gaussian whose width was set equal to the resolution of the NaI detector for the energy corresponding to the bin. The unfolded spectrum consists of a 66% confidence interval at 125 energies covering the gamma-ray energy range 0.69 to 10.6 MeV. Units are the number of gamma rays per unit energy per unit solid angle emitted in the direction of the detector. The ^{226}Ra unfolded pulse-height spectrum is compared in Figure 4 with values of relative intensity obtained by "smearing" the discrete-line intensities with gaussian functions corresponding to the window functions used in the unfolding. The visual comparison is quite good, as the largest errors are for the smallest relative intensities. The only large variances occur for E_γ between 0.95 and 1.0 MeV, and it is by no means certain that the error lies solely in the NaI measurement and analysis. It is apparent, though, that after grouping the gamma-ray data into 0.24-MeV energy intervals (as will be discussed below when comparing our data with prior work) the uncertainties due to measured response functions and unfolding methods will be small, at least for smaller gamma-ray energies. Results similar to those shown in Figure 4 were obtained for sources of ^{56}Co and ThC".

Because of the lead shield around the NaI detector, the background due to natural radioactivity was very small and contributed little to the counting rate during the period of observation which lasted only a few microseconds after each accelerator pulse.

Data were accumulated in 12-hour runs with the iron sample alternating with "background" measurements. As will be discussed below, "background"

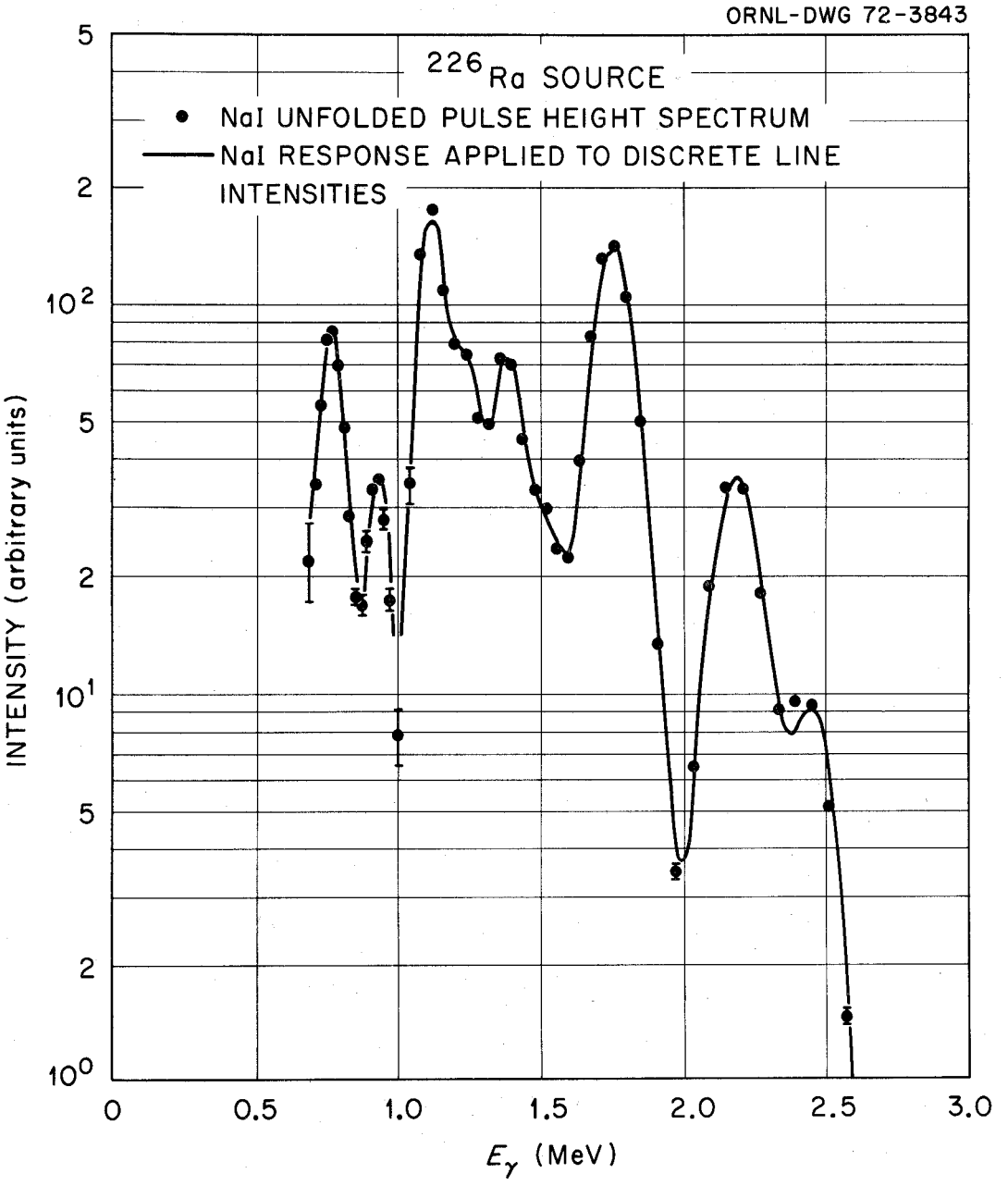

Fig. 4. Unfolded pulse-height spectrum for ^{226}Ra compared with intensity obtained by smearing discrete-line intensities with a Gaussian function corresponding to the intrinsic resolution of the NaI detector.

measurements are obtained by placing a 5.1-cm lead shadow bar between the sample and the NaI crystal just outside the LiH shield in front of the collimator, as shown in Figure 1. Similar runs were made for a carbon sample and a beryllium sample. The Be sample was used because, for $4 \leq E_n \leq 11$ MeV, there are no gamma rays reported known due to n+Be reactions.[3,15,27,28]

As usual in such experiments the background contributions to the pulse-height spectra cannot be measured directly and must be estimated on the basis of various assumptions for which only plausible a priori arguments can be given. Extensive investigations were made to develop a method of estimating the background counts in this experiment. Without any sample in the neutron beam, the counting rate in the detector was very small, about 1% of the sample-in counting rate. These counts were most likely due to air scattering of neutrons into the detector shield. Some of these scattered neutrons, and/or gamma rays produced by them, reached the detector despite the heavy shielding. When the sample is placed in the neutron beam, the background contribution must increase due to the additional neutron scattering in the room, and in particular, into the shield and detector. The pulse-height distribution as well as the time distribution of the background counts must depend on the angular and energy distribution of the neutrons emitted by the sample as a function of time. The presence of gamma rays from the sample prevents the measurement of this background. However, a lead shadow bar placed between the sample and the detector will strongly affect the detection of gamma rays from the sample but not nearly so

strongly the background due to neutrons incident on the shield. The size of the lead shadow bar was dictated by the requirement that it needed to shield the NaI detector from gamma radiation emanating only from the sample. As can be seen from Figure 1, this size shadow bar covers only a small fraction of the total front face of the shield. The thickness of the shadow bar must be a compromise between the need to attenuate substantially the gamma rays from the sample without seriously perturbing the incident neutron field, especially since the shadow bar will also shield the detector and its immediate environment from sample-scattered neutrons. We used a 5.1-cm thickness, a conveniently available size. For this thickness there is at most a 9% transmission of gamma radiation from the sample (for $3 \leq E_\gamma \leq 4$ MeV) based on the lead photon absorption cross sections. However, for this thickness of lead, one may calculate, on the basis of the neutron total cross section, that only about half of the neutrons hitting the shadow bar will strike the LiH shield uncollided. However, about half of the total cross section is due to elastic scattering which is dominated by small-angle scattering. The changes in energy and direction introduced by the lead elastic scattering on about half of the neutrons interacting with the shadow bar may not be very important in view of the 25-cm-thick LiH slab which follows it. For the remaining 50% of the neutrons interacting with the lead however, there is a very substantial degradation in energy due to (n,n') and (n,2n) interactions as well as reemission of neutrons away from the shield. This perturbation of the lead shadow bar on the background had to be investigated. In order to do so we used a beryllium sample. Runs were made with the Be sample in the beam with and without the lead shadow bar. The

gamma-ray pulse-height spectra were compared as a function of flight time (i.e, incident neutron energy), and within statistical uncertainties, no differences in the shape of the spectra $\{N(E_\gamma)$ vs $E_\gamma\}$ were observed except for a very small E_γ = 2.61 MeV peak in the lead-in measurement for E_n > 3 MeV. This peak was attributed to neutron inelastic excitation of the first excited state in ^{208}Pb. The ratio of the counting rate shadow-bar-in/shadow-bar-out was found to be 0.82. This ratio, which gives some measure of the perturbation of the lead on the background measurement, was studied as a function of time-of-flight and found to be constant. No explanation was found as to why this ratio is independent of incident neutron energy. A carbon sample was also used to test the background. For flight times corresponding to neutron energies below 4.8 MeV (threshold for inelastic scattering), the same ratio of 0.82 was obtained for the shadow-bar-in/shadow-bar-out ratio of counting rates. No change could be detected in the pulse-height distribution either. For flight times corresponding to $E_n \geq 4.8$ MeV and for pulse heights above 5 MeV, we tried to verify this ratio in the case of the carbon sample. This ratio was poorly determined because of the poor counting statistics and appeared to decrease at the highest neutron energies where it could have been as low as 0.4. However, this decrease could be explained in the case of carbon if there were some high-energy gamma rays. Since our pulse-height spectrum did not extend to 15 MeV, we could not positively ascertain if this was the case. It is possible also that the 5.1 cm of lead perturbs the background more for high-energy neutrons, even though this was not found to be the case with the beryllium sample. In view of the data at hand, we felt justified in keeping to 0.82 the ratio of

the magnitude of the background for shadow-bar-in/shadow-bar-out at all energies but increased the uncertainty in this ratio from 20% at low neutron energies to 50% at the highest energies. These errors were included in the background subtracted data before unfolding and propagated throughout the analysis. Therefore our method of subtracting the background, by using a constant ratio of 0.82, may be systematically underestimating it at the higher energies, but the errors in the resulting data should take into account this possibility.

Our procedure for analyzing the data consisted of adding together the TOF-PH arrays of all runs for a given sample configuration (i.e, iron sample with either shadow-bar-in or shadow-bar-out). Frequent calibrations in both pulse-height and time-of-flight showed negligible variations during the course of the measurement.

The next step was to form pulse-height distributions for various neutron energies by integrating the pulse-height spectra over time-of-flight. In our experience the unfolding procedure works well only if the statistical uncertainties are small ($\leq$3%). This necessitated summing over a sufficient number of time-of-flight channels to get adequate statistics in the pulse-height spectrum. Based on the need for statistical accuracy and smoothness of the yield curve, the decision was made to bin the data in neutron energy intervals of 0.2 MeV for E_n between 0.6 and 1 MeV, 0.5 MeV for E_n between 1 and 10 MeV, 1 MeV for E_n between 10 and 16 MeV, and 2 MeV for $E_n > 16$ MeV. A second data reduction was made using neutron energy intervals identical to those of GRT[6] to allow a direct comparison of the experiments.

The spectra obtained with the lead shadow bar were corrected by the factor 0.82 and subtracted from the spectra obtained without the shadow bar. One such example of spectra is given on Figure 5 for $5.15 \leq E_n \leq 6.15$ MeV together with some response functions for the detector. The channels of these pulse-height distributions were then grouped together into a series of bins corresponding to the structure of the response matrix. (The number of pulse-height channels per bin varied from 1 to 8.). The binned data with errors were then unfolded with the code FERD using the response matrix previously described. The data were then corrected for the transmission of the gamma rays through the lead shadow bar and for neutron and gamma-ray attenuation in the sample. The final results for the $5.15 \leq E_n \leq 6.15$ MeV neutron energy interval are shown in Figure 6. The sensitivity of the spectrometer is clearly indicated in this figure; note that gamma rays having $E_\gamma > 6.15$ MeV are observed. We believe that these are real and are due to fast-neutron capture in Fe, for which reaction the cross section is ≈ 1 mb for $E_n \sim 5$ MeV (Ref. 7, 13).

Our NaI unfolded data yielded close to 4000 data points. It is impractical to publish these numbers with the paper. The numerical values of the data are collected in a separate report.[29] In an attempt to reduce the bulk of the data, we have grouped the gamma rays into 240-keV intervals to facilitate comparison with the data of reference 6. The numerical tables are relagated to the appendix. This very coarse binning of the NaI gamma-ray data does not do justice to the fine structure possible with the NaI spectrometer as evidenced on Figure 6.

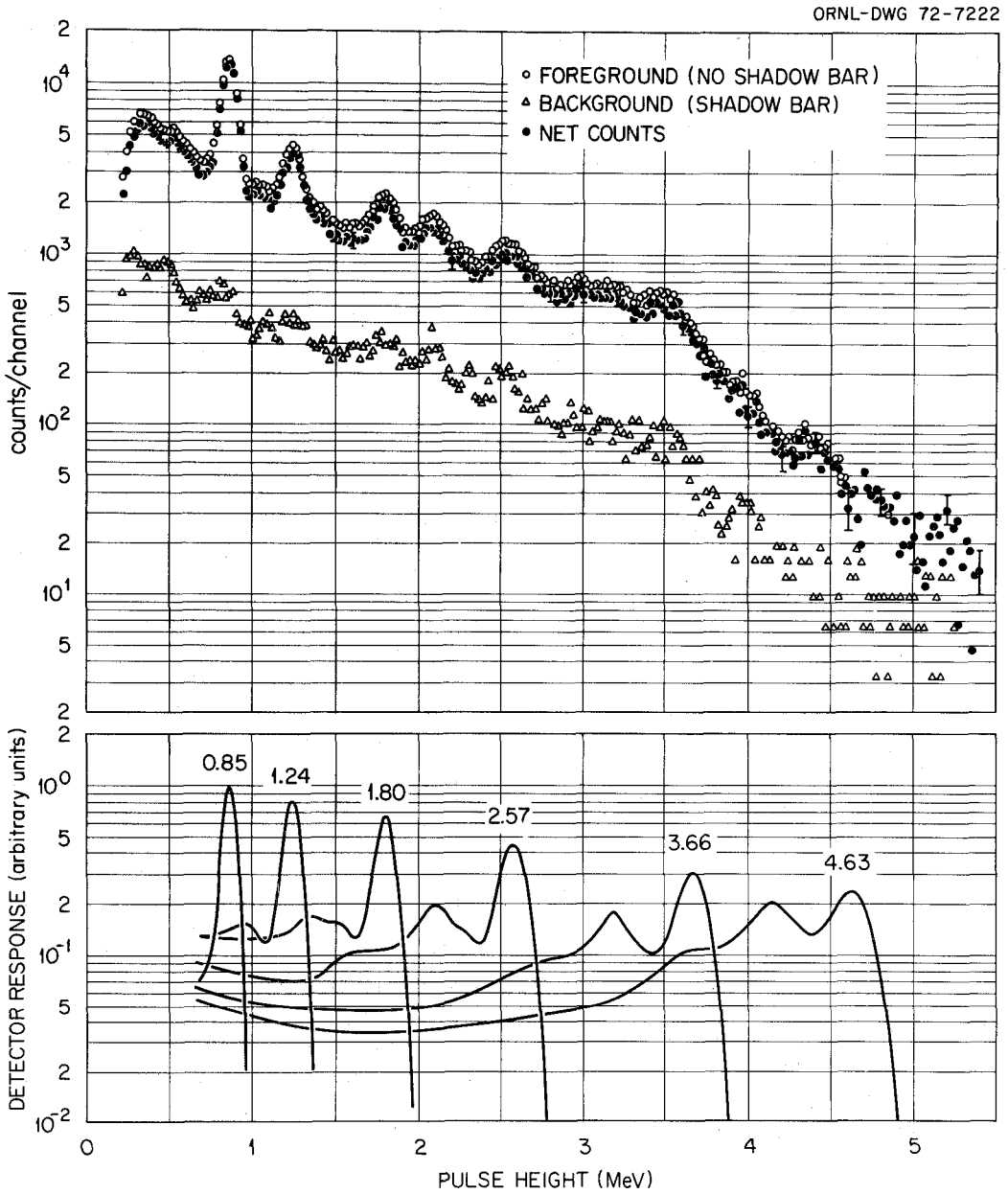

Fig. 5. Gamma-ray pulse-height spectra produced by 5.14 to 6.13 MeV neutron interactions with iron. The background spectrum obtained by placing the 5.1 cm lead shadow bar in front of the collimator. The curves shown at the bottom of figure are some of the response functions for the NaI detector.

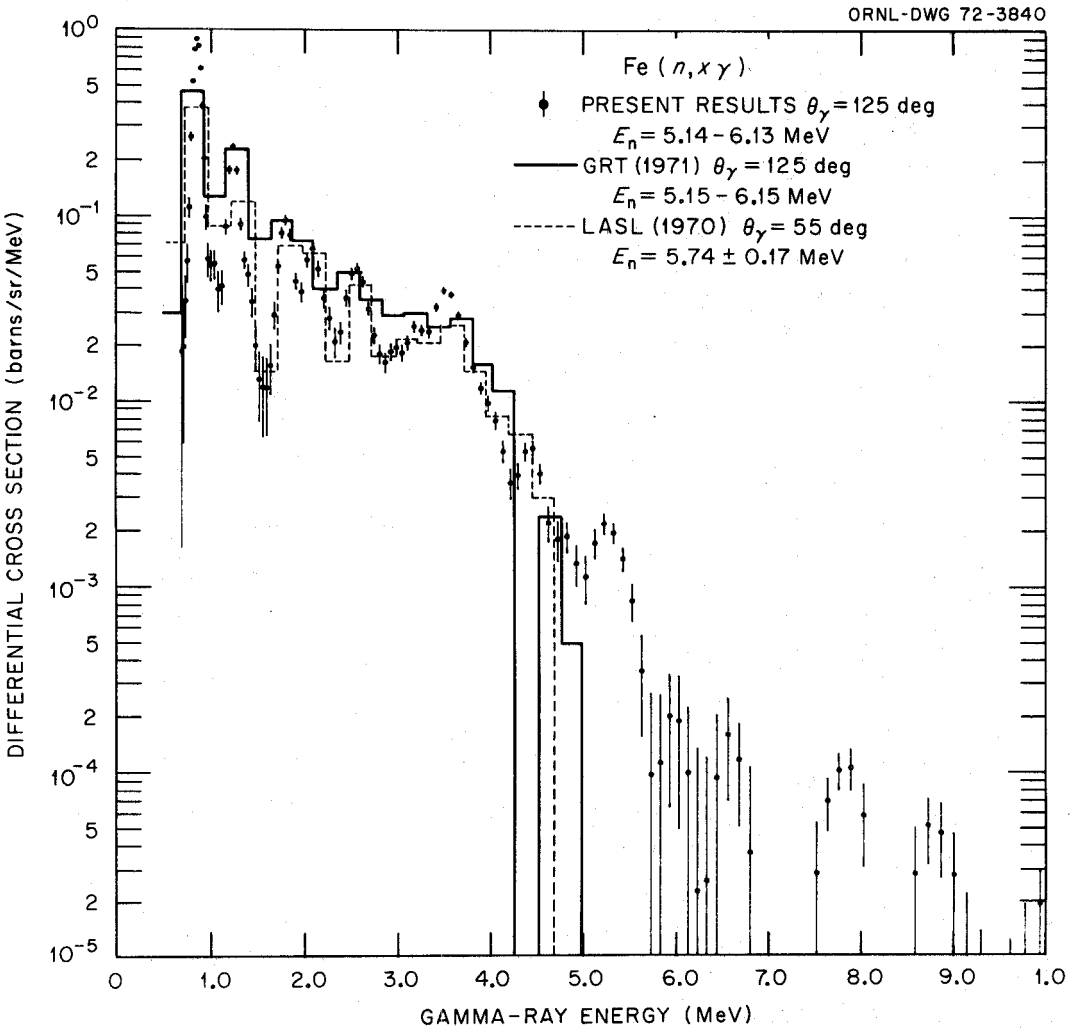

Fig. 6. Differential cross sections for gamma rays produced by 5.14- to 6.13-MeV neutron interactions with iron. The present results are compared with similar data reported by Drake et al., (LASL (Ref. 3) and Orphan et al., GRT (Ref. 6).

B. Ge(Li) Experiment

The Ge(Li) experimental system has been reported several times in detail.[14,15,30] The incident neutrons (monoenergetic and pulsed, generated using a Van de Graaff accelerator) interacted with a 30 g sample of natural iron in the form of a right circular cylinder. Spectra were obtained at ~0.5-MeV intervals for E_n between 5.35 and 9.0 MeV using the 30-cm^3 detector described in prior reports.[14,15] For all E_n data were obtained at θ_γ = 55 and 90 deg and for several E_n at θ_γ = 35 and 75 deg. Additional spectra were obtained for E_n = 4.85 and 7.0 MeV at θ_γ = 125 deg using a large detector (45 cm^3) and an improved experimental arrangement (see Ref. 10). Fast-timing electronics were used to discriminate against most unwanted background events so that the resulting spectra contained data primarily due to prompt n + Fe interactions. Detector calibration and corrections due to multiple scattering and finite sample size followed methods discussed previously.[14,15] The absolute calibration of the beam monitoring system is believed reliable to ±7% (Ref. 15).

The spectrum obtained for E_n = 4.85 MeV is shown schematically in Figure 7. In this figure the shaded band indicates the underlying Compton distribution, and the peaks indicate the shapes observed. Note that some of the peaks corresponding to high-energy gamma rays are not Gaussian shaped and are broad. This is due to Doppler broadening, i.e., the decay of the excited Fe ion while still in motion. Experience has shown that very nonsymmetric peak shapes may be observed,[15,31] and it is not always certain that a given broad peak is due to more than one gamma ray. In addition, the measured gamma-ray energies were shifted from the true gamma-ray energies up to 0.15% of the true gamma-ray energy. The actual amount of energy shift

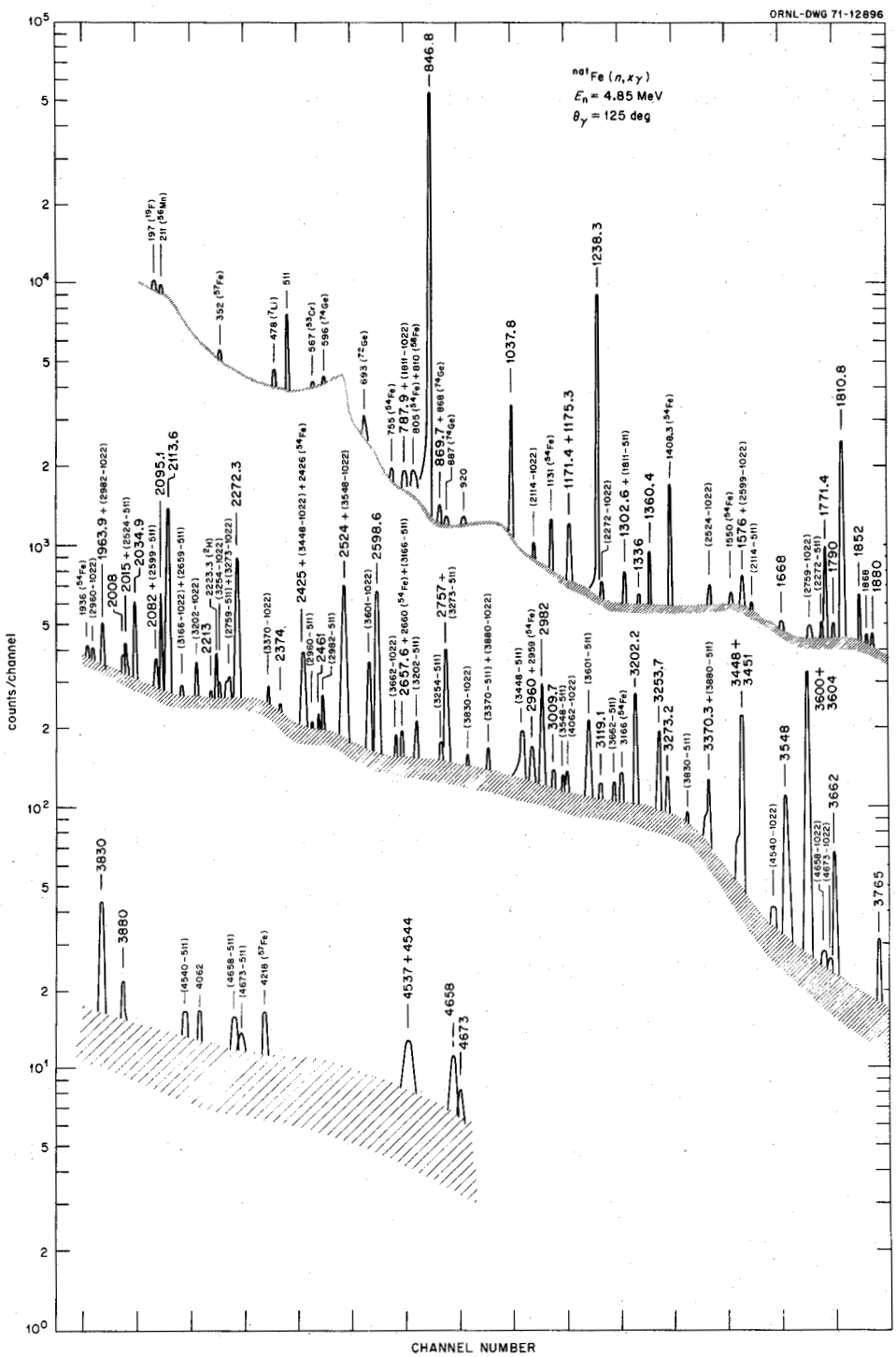

Fig. 7. Gamma-ray spectrum for the Fe(n,xγ) reaction at E_n = 4.85 MeV, $\theta_\gamma = 125^o$. Each whole segment has 750 channels. Peaks corresponding to transitions in ^{56}Fe are indicated by the larger labels. Peaks known to be due to other nuclei are indicated by isotope symbol. Full energy peaks are labelled with the gamma-ray energy; escape peaks are labelled with (E_γ - 511) and (E_γ - 1022) for the single- and double-escape modes, respectively.

depends upon the lifetime of the emitting state and these are not always known. All of the spectra were carefully studied to relate observed gamma-ray peaks with inelastic-scattering transitions to obtain branching ratios for levels where these are not known.

The best spectrum for this study is the one shown in Figure 7, and an attempt was made to identify the sources for all gamma rays observed. Placement of the gamma rays among known levels in ^{56}Fe depended upon previously determined excitation energies,[32] especially since the gamma-ray energies could not be determined to better than 3 keV for the highest energy gamma rays. The gamma-ray energy calibration for this spectrum utilized previously determined accurate gamma-ray energies[8,33] corrected for excited state lifetimes when known[34] using Blaugrund's methods.[35] The results of this analysis are presented in Table 1. All transitions corresponding to $E_x \geq 4.4$ MeV are either new or support previous tentative assignments. Study of spectra for $E_n = 5.4$ MeV yielded a number of additional gamma rays having small differential cross sections (generally < 0.2 mb/sr). Only 3 of these could unambiguously be assigned as transitions among levels in ^{56}Fe. These were $E_\gamma = 4049$ keV assigned to the 4875-846 keV transition and ground-state transitions from levels with $E_x = 5228$ and 5255 (± 3) keV. A few higher energy gamma rays were observed in the spectra obtained for $E_n \geq 6$ MeV; those observed had very small yields and they could not be reliably assigned to specific transitions among known levels in ^{56}Fe.

Absolute values of $d\sigma/d\omega$ were extracted from the spectra in the same manner as previously discussed.[14,15] The major uncertainties associated with reduction of these data were related to (a) the large number of gamma rays observed, which resulted in increasing the underlying Compton distribution, and (b) especially at the higher bombarding energies the effect of

TABLE 1. GAMMA RAYS FROM 4.85-MeV NEUTRON INTERACTIONS WITH $^{56}Fe(\theta_\gamma=125$ DEG, $\Delta E_n=0.15$ MeV)

E_γ [a]	I_γ [b]	Assignment [c]	E_γ	I_γ	Assignment
787.9	0.5±0.3	3445.4-2657.6	2461	0.22±0.12	4546-2085.1
846.8	89.0 ±4.5	846.8-g.s.	2523.5	4.60±0.42	3370.3-846.8
869	0.25±0.12	3829-2960.4	2598.6	4.45±0.31	3445.4-846.8
1037.8	5.53±0.40	3122.9-2085.1	2657.6 [d]	0.2±0.1	2657.6-g.s.
1171.4 }	2.20±0.30	3829-2657.4	2757 [e]	3.8±0.3	3604-846.8
1175.3 }		4298.2-3122.9	2960.4 [d]	0.2±0.1	2960.4-g.s.
1238.3	20.0 ±1.1	2085.1-846.8	2982	2.13±0.18	3829-846.8
1302.6	0.82±0.25	3387.7-2085.1	3009.7	0.25±0.11	3856.5-846.8
1336	0.29±0.15	4458-2960.4	3119.1	0.32±0.11	3119.1-g.s.
1360.4	1.51±0.16	3445.4-2085.1	3202.2	2.03±0.16	4049.0-846.8
1575	0.40±0.20	4694-3119.1	3253.7	1.12±0.11	4100.5-846.8
1668	0.20±0.12	3753-2085.1	3273.2	.46±0.10	4120.0-846.8
1771.4	2.67±0.28	3856.5-2085.1	3370.3	.74±0.20	3370.3-g.s.
1790	0.23±0.12	4447-2657.6	3448 }	3.05±0.35	3448-g.s.
1810.8	10.4 ±0.60	2657.6-846.8	3451.4 }		4298.2-846.8
1852	1.06±0.15	4509-2657.6	3548	1.67±0.10	4395-846.8
1880	0.36±0.15	4537-2657.6	3600 }	3.85±0.20	4447-846.8
1963.9	0.43±0.14	4049-2085.1	3604 }		3604-g.s.
2008	0.42±0.22	4093-2085.1	3662	0.67±0.10	4509-846.8
2015.4	0.65±0.22	4100.5-2085.1	3765	0.24±0.09	4612-846.8
2034.9	1.79±0.15	4120.0-2085.1	3829 }	0.53±0.09	3829-g.s.
2082	0.51±0.14	4740-2657.6	3830 }		4673-846.8
2095.1	2.03±0.14	2941.9-846.8	3880	0.19±0.08	4727-846.8
2113.6	7.28±0.40	2960.4-846.8	4537 }	0.32±0.08	4537-g.s.
2213	0.14±0.10	4298-2085.1	4544 }		4544-g.s.
2272.3	4.98±0.30	3119.1-846.8	4658	0.24±0.09	4658-g.s.
2374	0.18±0.12	4459-2085.1	4673	0.11±0.07	4673-g.s.
2425 [d]	0.83±0.22	4509-2085.1			

[a] $\Delta E_\gamma=0.08\%$, due principally to uncertainties in Doppler shift corrections.

[b] Elemental differential cross sections (mb/sr) not corrected for isotopic abundance.

[c] Other lines observed due to interactions of neutrons with ^{nat}Fe include: 211-keV from $^{56}Fe(n,p)^{56}Mn$, $I_\gamma=0.13\pm0.07$ mb/sr; 352-keV from $^{57}Fe(n,n')^{57}Fe$ and $^{56}Fe(n,\gamma)^{57}Fe$ seen in background, $I_\gamma=0.6\pm0.2$ mb/sr; 567-keV due to $^{56}Fe(n,\alpha)^{53}Cr$, $I_\gamma=0.25\pm0.12$ mb/sr; and several transitions due to $^{54}Fe(n,n')^{54}Fe$.

[d] Coincident with gamma rays due to excitation of ^{54}Fe(5.8% isotopic abundance in sample).

[e] May include 2752-KeV gamma associated with 3599-846.8 keV transition.

Doppler broadening, which resulted in reduced apparent energy resolution. The combined uncertainty in cross sections resulting from all of the other parameters (e.g., geometrical corrections, detector efficiency, etc.) is estimated to be < 10%. Numerical values of the absolute differential cross sections and associated uncertainties are collected in the separate report[29] mentioned above.

C. Experimental Results for n + ^{54}Fe

In all the high-resolution spectra a number of peaks were observed which could not be related to known transitions due to n + ^{56}Fe. Experimental determination of the order of magnitude of gamma-ray yields in ^{54}Fe(n,xγ) would assist in gamma-ray identifications, since the isotopic abundance of ^{54}Fe is 5.8%. Four spectra were obtained using the improved Ge(Li)-spectrometer system mentioned above[10] for a 48 g sample enriched to >97% in the ^{54}Fe isotope. Data were obtained for E_n = 4.85, 5.4, and 6.45 MeV at θ_γ = 125 deg, and for E_n = 5.92 MeV at θ_γ = 55 deg. The spectrum obtained for E_n = 5.4 MeV is shown in Figure 8.

In addition to obtaining gamma-ray production cross sections, which are tabulated in Ref. 29, the four spectra were studied for spectroscopic information about the ^{54}Fe nucleus, and the results of this study are summarized in Figure 9. The "branching" ratios shown in parentheses in this figure are actually ratios of cross sections at θ_γ = 125 deg. These ratios are in reasonable agreement with prior information (see Ref. 36) except for the 1509 keV transition from the 4048-keV state. The present value of 25% is much larger than the 2% given in Ref. 36, suggesting that the observed peak includes another transition. At E_n = 5.4 MeV the peak corresponding to E_γ = 3.29 MeV is clearly a doublet having energies 3288

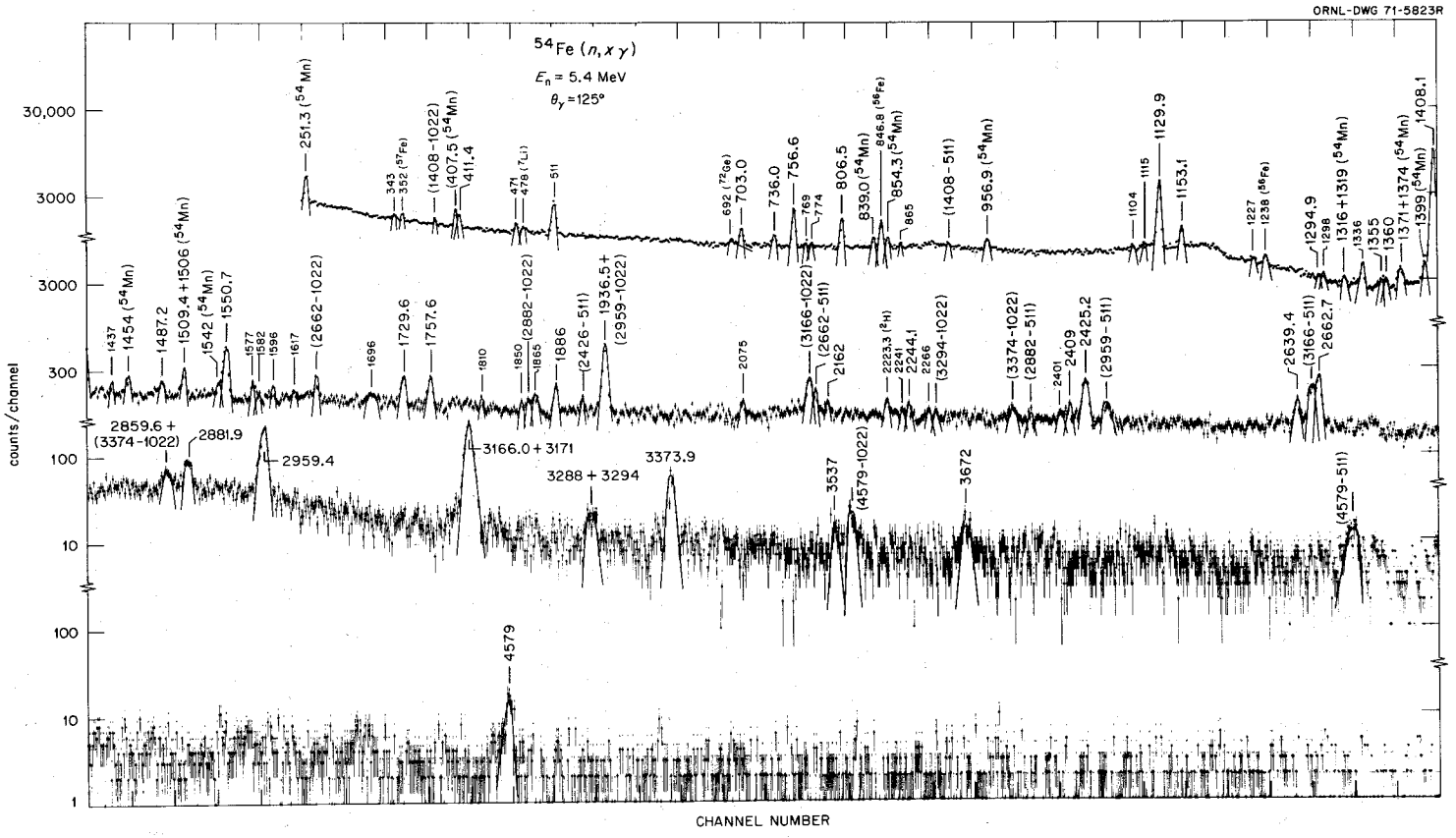

Fig. 8. 4096-channel spectrum of γ rays for 5.4-MeV neutron bombardment of ^{54}Fe, θ_γ = 125 deg. Peaks are labelled with the energy of the detected γ ray. Escape peaks are indicated by (E_γ - 0.511) and (E_γ - 1.022) labels. Isotope symbols indicate γ radiation emanating from nuclei other than ^{54}Fe. The contributing nuclear species for some of the observed gamma rays could not be determined; these peaks are indicated by smaller labels.

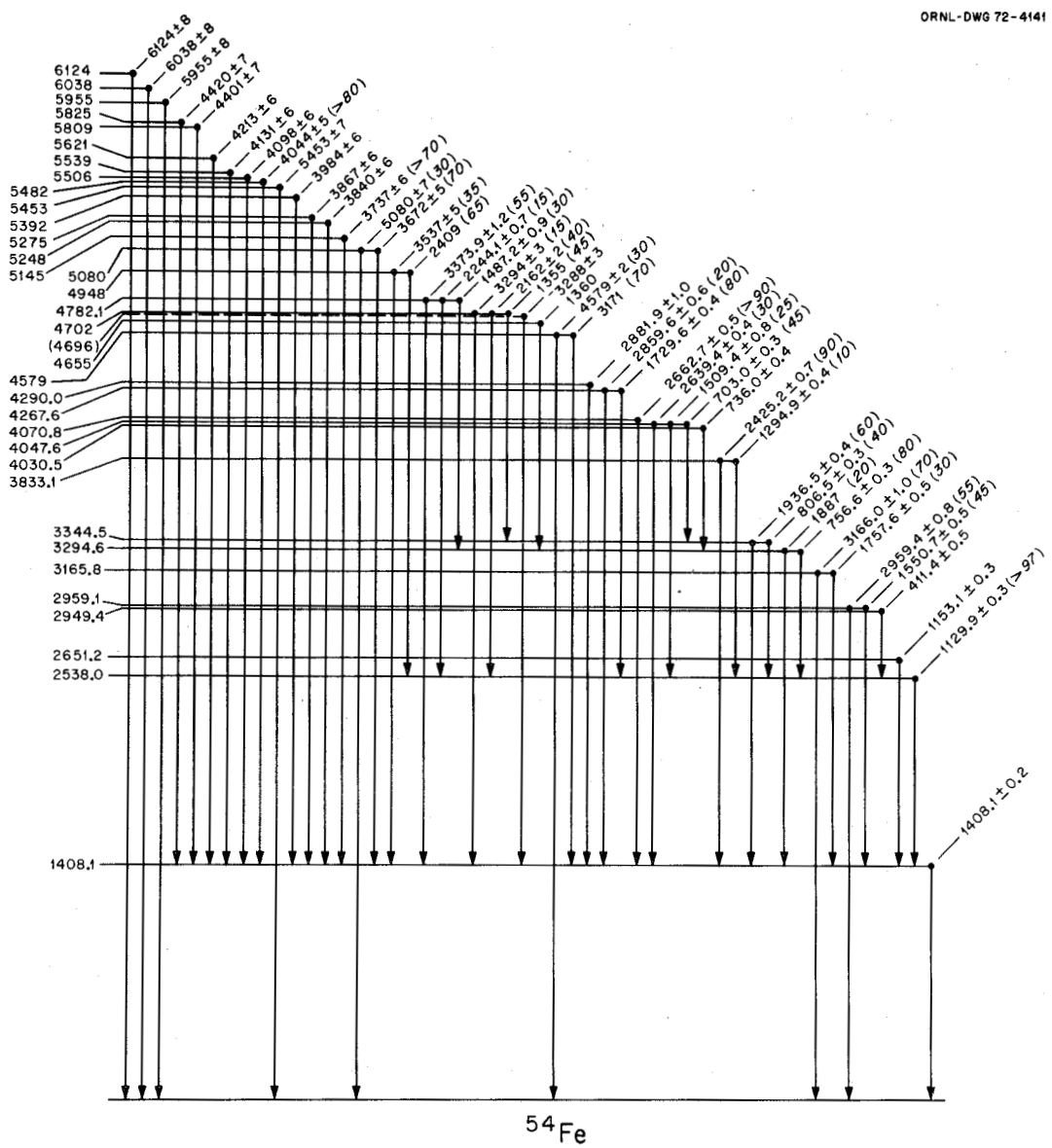

Fig. 9. Level structure of ^{54}Fe deduced from present results. Transitions are labelled by $E_\gamma \pm \Delta E_\gamma$ (branching ratio), with E_γ in keV and branching ratio in %. The ΔE_γ for E_γ > 3700 keV are due primarily to uncertainties in Doppler shift determination because of lack of information on the lifetimes of the excited states. Transitions without ΔE_γ indicate gamma-ray energies which could not unambiguously be determined. "Branching" ratios are ratios of cross sections for θ_γ = 125 deg and are averages for all values obtained.

and 3294 keV and about equal in intensity, suggesting (by the dashed line in Figure 9) another energy level in ^{54}Fe nearly degenerate with the 4702-keV state. In addition, new information concerning the reaction $^{54}Fe(\underline{n},\underline{p}\gamma)^{54}Mn$, which has a large cross section ($\geq$ 400 mb for E_n = 5.4 MeV), was obtained from study of these data.[37] Although a more thorough study of $\underline{n}$ + ^{54}Fe reactions would be interesting, the basic purposes were satisfied. Reasonable estimates can be made to the total gamma-ray production yield of the effect of neutron interactions with ^{54}Fe.

D. Excitation of the 846-keV Level in ^{56}Fe Near Threshold

Recently, Voss *et al.*[12] and Perey *et al.*[38] have reported measurements which demonstrate that near threshold the excitation function for the production of the 846-keV gamma ray exhibits pronounced resonant structure, more so than had previously been observed[6,7] or expected. Since other nuclei have resonant structure in excitation functions for inelastic scattering[6,12,38] we were interested in ascertaining if the present NaI-spectrometer system could be used to determine such structure. Therefore a run was made to repeat the 846-keV gamma-ray cross-section measurements for E_n between 0.8 and 2 MeV. The same experimental arrangement described in Section IIA above was used, except that the beam pulse width was reduced to 5 nsec. Since only one gamma ray was involved (and since unfolding several hundred spectra was a large task), the data-taking routine was changed as follows: a window was set about the peak corresponding to the 846-keV full-energy peak in the pulse-height spectrum and a 2048-channel TOF spectrum was obtained for pulse heights in the window; a second window of the same size was set in the pulse-height spectrum just above the 846-keV peak and a second 2048-channel TOF spectrum was obtained.

The total running time was 40 hours. The second TOF spectrum was subtracted from the first to provide a relative set of cross sections. These were integrated and then normalized to production cross sections obtained as described above in Section IIA. The results for $E_n < 1.35$ MeV are shown in Figure 10 and compared with data of Voss et al.[10] (Karlsruhe) and GRT.[6] Although the present results do not have quite as good a neutron energy resolution as the Karlsruhe results, we feel that the system is capable of comparable results should the need arise. For Fe the Karlsruhe results (corroborated by the report of Ref. 38) appear to be quite reliable.

III. DISCUSSION AND COMPARISON OF DATA

The data may be considered to belong to two categories. In the first category we consider $d\sigma/d\omega$ values for discrete individual gamma rays; in the second we consider $d\sigma/d\omega$ values for binned-group data, i.e., the sum of $d\sigma/d\omega$ for all discrete individual lines having E_γ within the specified bin limits. The recent reports using Ge(Li) spectrometers have concentrated on the first category and the data have proved useful in nuclear structure studies. For shielding calculation purposes, however, the second category is the preferred format and evaluated gamma-ray files are usually prepared in similar format. Therefore, the NaI spectrometer and data-reduction system described above was developed as an efficient system for obtaining cross-section data of the second category.

A. Comparison of E_γ = 846-keV Data

The 846-keV gamma ray is the strongest line observed (see Figure 6) and makes up more than 97% of the discrete gamma-ray yield in the

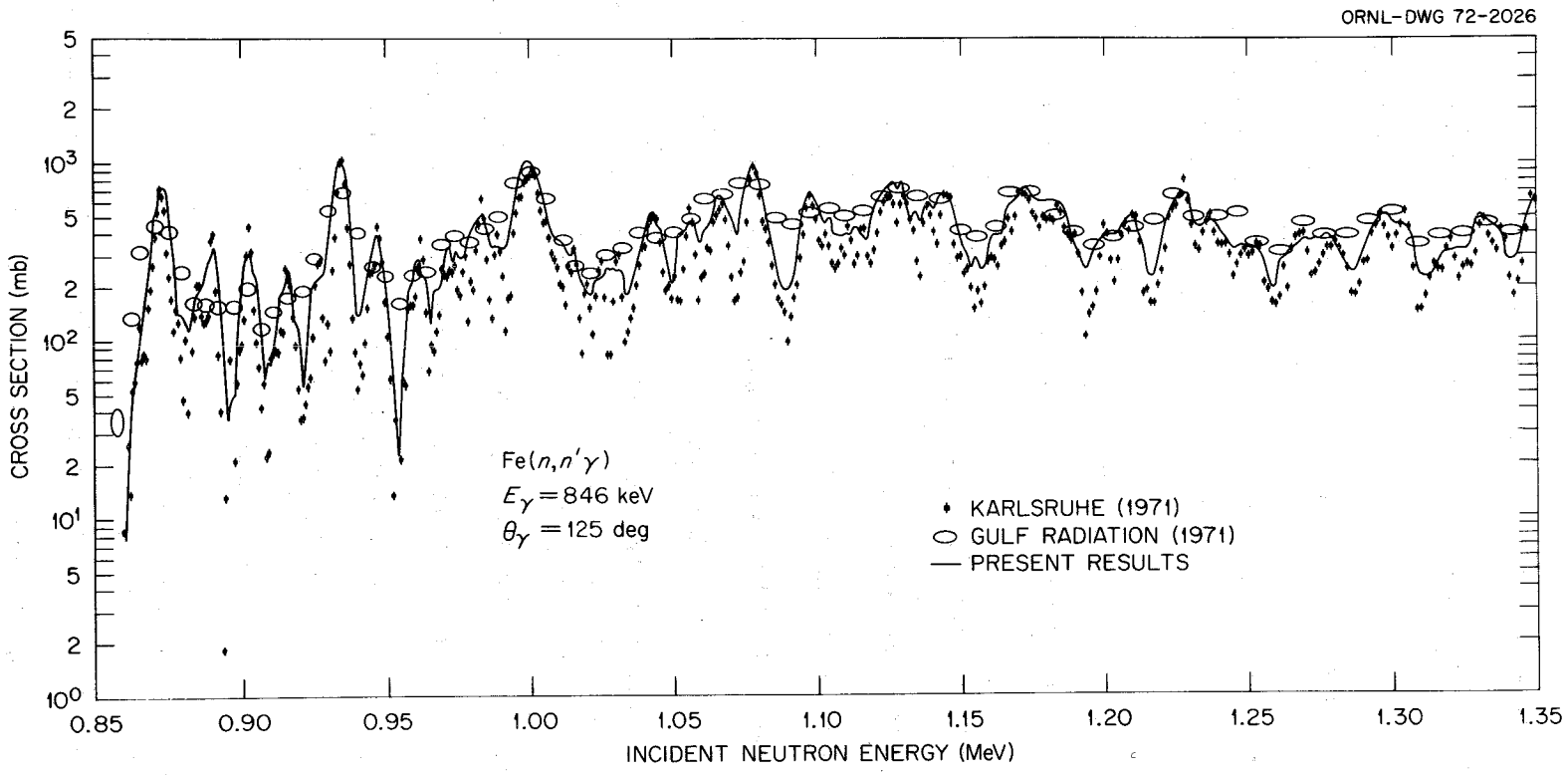

Fig. 10 Excitation function for the production of the 846-keV gamma-ray in ^{56}Fe. The present data are compared with similar data reported by Orphan et al., Gulf Radiation (Ref. 6) and Voss et al., Karlsruhe (Ref. 12).

$708 \leq E_\gamma \leq 946$ keV bin,[39] at least for $E_n < 9$ MeV, according to our Ge(Li) measurements. Comparison of our data for this E_γ bin with those of TNC,[2] LASL,[3] and GRT,[6] and the ENDF/B-III gamma-ray file[13] is shown in Figure 11. There are some obvious disagreements among the various sets of data. Our data agree very well with the two LASL data points at $E_n = 4$ and 5.7 MeV, but their data is higher by 35% for $E_n > 6.0$ MeV. No such behavior in the cross section seems indicated by the two sets of continuous neutron-energy measurements, ours and GRT's. Except for the point for $4.10 < E_n < 5.15$, the GRT data are approximately 10% higher at all energies. The TNC measurements seem to support our lower cross-section values below 2 MeV and GRT's higher values between 3 and 4 MeV, although there the TNC error bars overlap the other two sets of data.

Figure 12 shows the comparison of our results with several Ge(Li)-spectrometer measurements for the energy region $4 < E_n < 10$ MeV. The shaded band represents the limits of our NaI-spectrometer data for the total E_γ bin of Figure 11, but all the remaining data[4-6] are for the 846-keV gamma ray only. Note that in this case the GRT data[6] agree well with the present NaI data even though we are comparing our total yield for $708 < E_\gamma < 346$ keV to their data for the 846 keV gamma ray only. Both ours and GRT's data were obtained using an electron linear accelerator to provide the neutron source; on the other hand the Obninsk,[4] CEA[5] and present Ge(Li) results employed Van de Graaff accelerators to produce neutrons. There is a distinct difference in the character of the excitation function, as the GRT and present NaI data peak for E_n about 5 MeV; whereas the Van de Graaff data continue to increase. All three of these experiments (Refs. 5 and 6 and present Ge(Li) data) used the $D(d,n)^3He$ reaction.

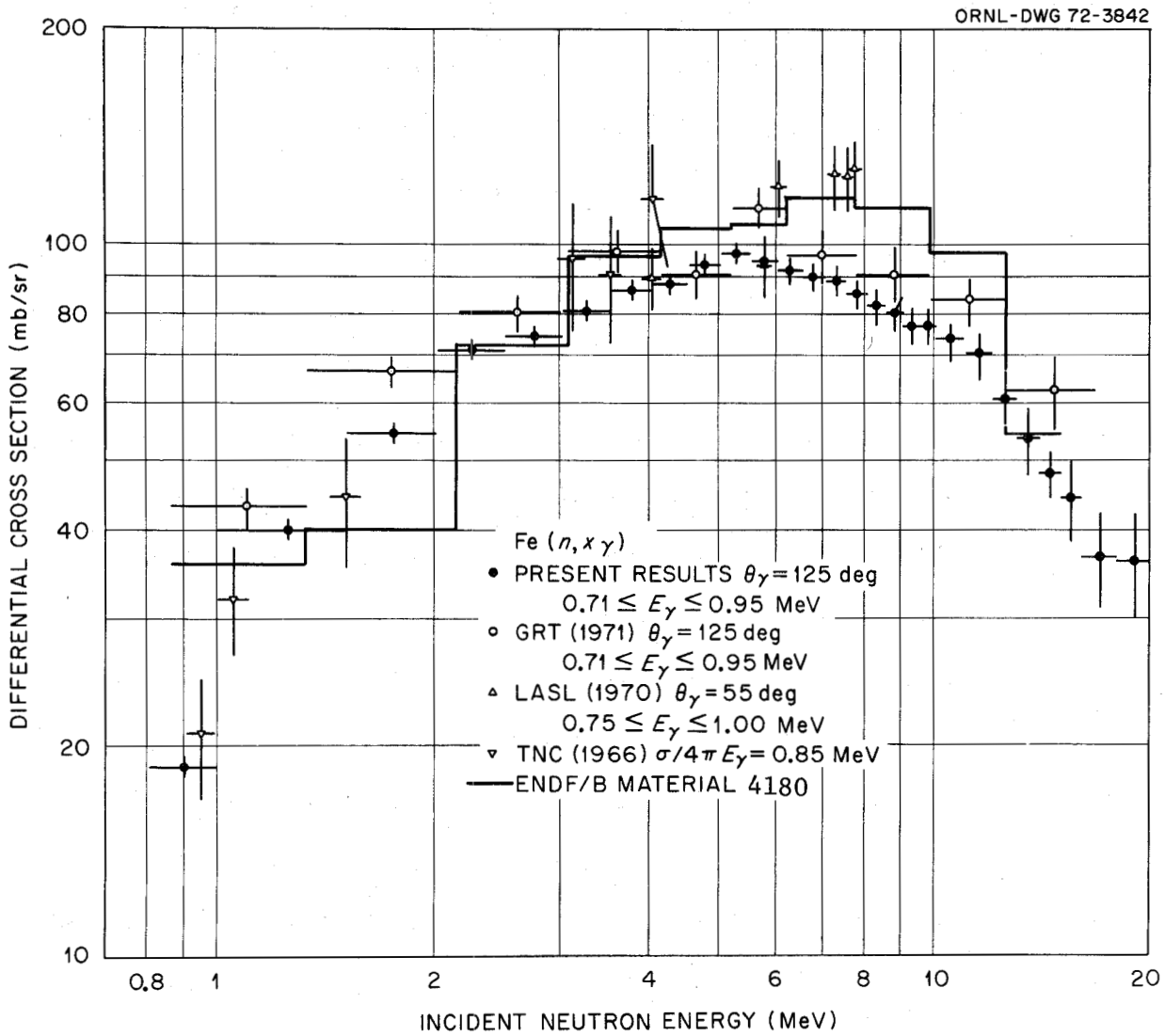

Fig. 11. Elemental differential cross sections for gamma rays due to the Fe(n,xγ) reactions for the gamma-ray energy bin between 0.703 and 0.946 MeV. The present NaI results are compared with data reported by the Los Alamos Group (Ref. 3), the Gulf Radiation Technology Group (Ref. 6), and with the current ENDF/B evaluation (Ref. 13).

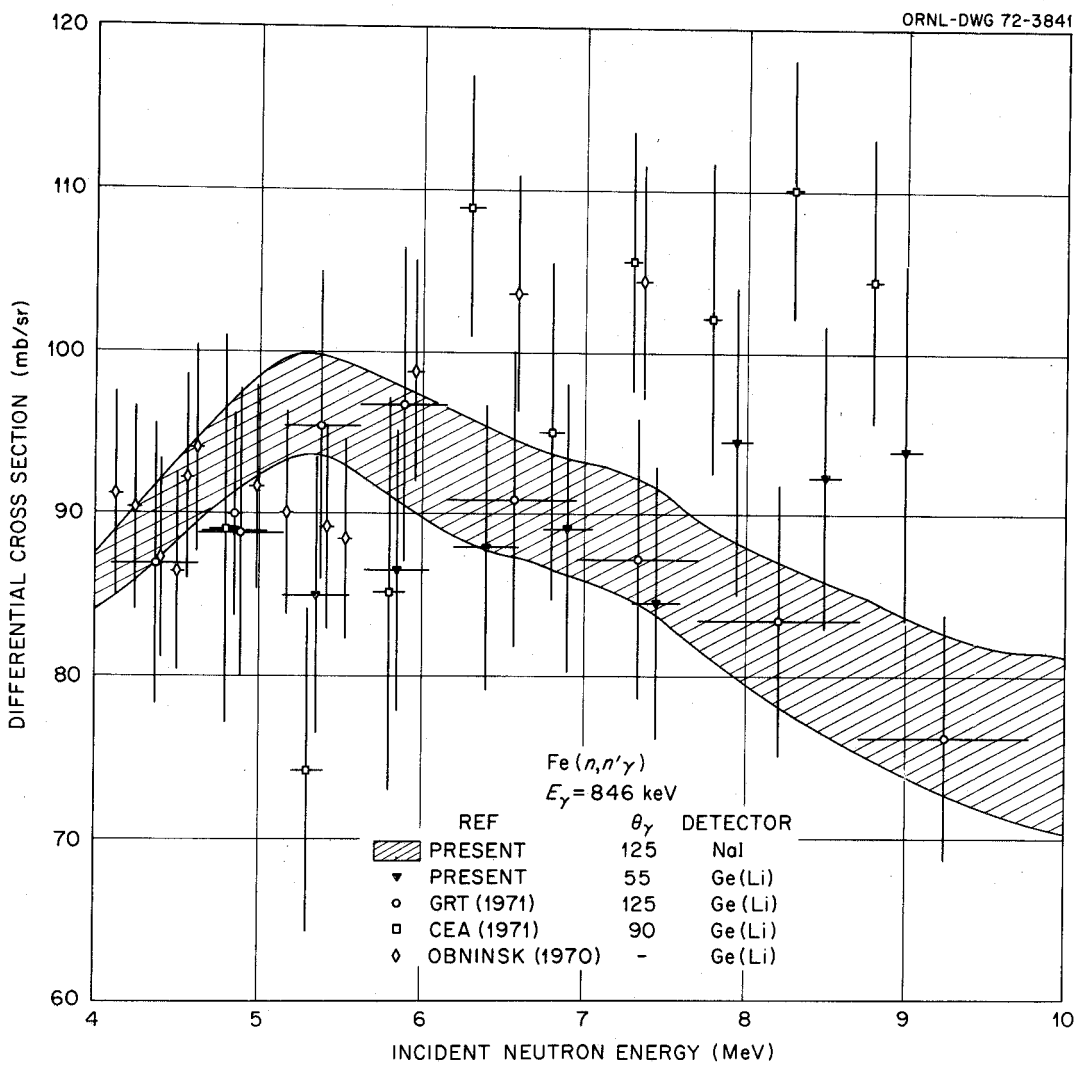

Fig. 12. Elemental differential cross sections for 846-keV gamma rays due to $^{56}Fe(n,n'\gamma)$ reactions. The present NaI binned-group data shown in Fig. 10 are here indicated by the shaded band. These data, and the present Ge(Li) results, are compared with data reported by groups at Los Alamos (Ref. 3), Obninsk (Ref. 4), Commissariat a l'Energie Atomique (Ref. 5), and Gulf Radiation (Ref. 6).

The three-body break up for this reaction which occurs for $E_d \geq 5$ MeV (i.e., such that $E_n \geq 8$ MeV for the two-body reaction) could not explain this apparent systematic behavior. Cross sections for the three-body break up[40] have been used to estimate the effect at 9 MeV which accounted for 7% of the observed gamma-ray production cross section in our data.[41] Although all of the data on Figure 12 may well be within the estimated systematic uncertainties of the experiments, most of the Van de Graaff data show a systematic large increase in cross sections slightly above 6 MeV and in this sense are similar to the LASL results[3] shown on Figure 11. However, there is a difference between the LASL data[3] and the other[4,5] Van de Graaff measurements. As will be shown later, all of the measurements are in good agreement for the 1238-keV gamma ray above 6 MeV except the LASL data which are also about 30% too high. Orphan et al.[6] conjecture that the LASL data include some contribution due to "continuum" gamma rays, but this could not explain the disagreement shown on Figure 11 since the GRT data and our NaI data are also supposed to include any "continuum" present.

To conclude on the comparisons for the 846 keV gamma ray, the GRT binned-group data[6] shown in Figure 11 are in very good relative agreement with our data, the only difference being that our data average ~10% lower at all energies. Our binned group data for $708 < E_\gamma < 946$ keV are in excellent agreement with their value for the 846-keV gamma-ray line, consistent with our estimate of the continuum contribution.

B. Comparison of E_γ = 1.24-MeV Data

The E_γ = 1.24 MeV gamma ray is the second strongest line observed in all spectra for E_n > 2 MeV. Comparison for our binned group data for 1185 < E_γ < 1424 keV with LASL,[3] GRT[6] and the ENDF/B evaluation appear similar to Figure 11 except that the GRT data instead of being 10% higher are closer to 50% higher. Comparison for the production of $d\sigma/d\omega$ for the 1.24-MeV gamma ray itself is shown on Figure 13. In this figure an estimate for this $d\sigma/d\omega$ was obtained from our NaI data by assuming that the yield in the spectra from 1.20 < E_γ < 1.31 MeV was proportional to the cross section at E_γ = 1.24 MeV. The constant of proportionality was obtained for 2 < E_n < 3 MeV and assumed constant for E_n > 3 MeV. Any error in this method of approximation, due to "continuum" gamma rays or a nearby gamma ray, should result in too large values for $d\sigma/d\omega$. As indicated in the figure, all of the data, except the LASL results,[3] are in reasonably good agreement. There is some scatter among the several data sets obtained with Ge(Li) detectors, particularly the Obninsk results.[4] Resonances in the excitation function may be expected, particularly near threshold, similar to those observed in Figure 10 for the 846 keV transition. However, none of the experimental results shown in Figure 13 appear to yield such information, except possibly the Obninsk results for which to our knowledge a complete report has not been published.[42] It is worth noting the different shapes of the cross sections as a function of energy for the 846 and 1238 keV lines. The abrupt reduction of $d\sigma/d\omega$ values for E_n above 12 MeV, for both the 846 and 1238 keV lines, very evident in our data, is related to the onset of the ^{56}Fe(n,2n) reaction (E_n threshold of about 12.7 MeV).

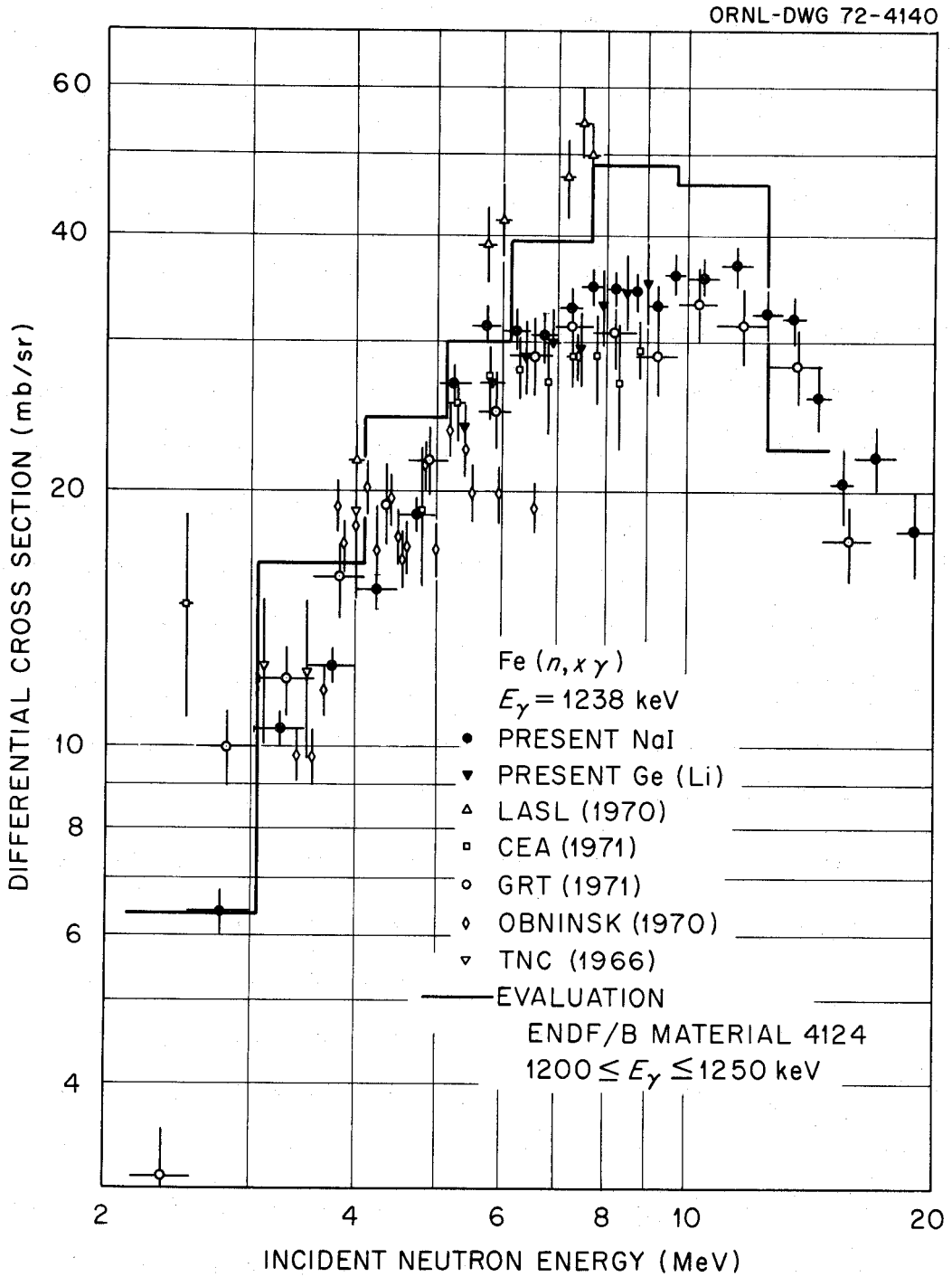

Fig. 13. Elemental differential cross sections for 1238-keV gamma rays due to $^{56}Fe(n,n'\gamma)$ reactions. The points labelled present NaI are estimates from the NaI data as described in the text. These data, and the present Ge(Li) results, are compared with data reported by groups at Texas Nuclear (Ref. 2), Los Alamos (Ref. 3), Obninsk (Ref. 4), Commissariat a l'Energie Atomique (Ref. 5) and Gulf Radiation (Ref. 6), and with the current ENDF/B evaluation (Ref. 13).

To conclude on the comparison of the two strongest lines of the iron data, the only ones we can confidently extract from our NaI data, there is generally 20% agreement among all the data sets.

C. Discussion of Remaining Gamma-Ray Data

Comparisons for other discrete-line data are similar to those shown on Figures 12 and 13, and comparisons for binned group data are somewhat similar to those shown in Figure 11. Orphan et al.[6] have made an extensive comparison of their line data with our Ge(Li) results on the basis of our preliminary data[41] and found good overall agreement. We shall, therefore, not repeat this comparison here. For the unfolded data the major trend, with a few exceptions, is toward better agreement for larger E_γ, partly accounted for by increased uncertainties. An indication of differences as well as agreements between the present NaI data and GRT results[6] is given in Table 2.

The "Σ lines" data are in good agreement (~15%), with the largest difference for the highest E_n bin. This difference is almost entirely accounted for by the high values for the 846 keV line discussed before. The "Partial" differential cross sections are in excellent agreement for $E_n < 10$ MeV, becoming very poor for $E_n > 12.5$ MeV. The "Total" differential cross sections are in fair agreement (~20%) for $E_n < 5.15$ MeV (except possibly for the $3.06 < E_n < 4.10$ MeV bin). However, the GRT "Total" data are 40% or more larger than the present NaI values for $E_n > 5.15$ MeV. In view of the overall agreement for discrete lines and for the "Partial" sums up to $E_n = 10$ MeV, the very large disagreement in the total gamma-ray yield deserves careful consideration.

TABLE 2. TOTAL AND PARTIAL GAMMA-RAY YIELDS (IN MB/SR) FOR θ_γ = 125 DEG.

E_n (MeV)	Total[a]		Partial[b]		Σ Lines[c]	
	GRT[d]	Present[e]	GRT	Present[e]	GRT	Present[f]
0.86-1.32	43	33			44	
1.32-2.14	71	58			68	
2.14-3.06	96	87			98	
3.06-4.10	185	139	9	10	148	
4.10-5.15	214	190	33	34	168	175(193)
5.15-6.15	318	229	52	48	187	172(194)
6.15-7.71	332	252	62	63	175	174(186)
7.71-9.78	338	252	74	78	158	183(188)
9.78-12.56	379	247	105	85	147	
12.56-16.74	326	174	92	54	106	

[a]Integrated yield for $E_\gamma \geq 0.71$ MeV.

[b]Integrated Yield for $E_\gamma \geq 2.38$ MeV.

[c]Summed $d\sigma/d\omega$ for the discrete lines reported by GRT.

[d]Ref. 6.

[e]Present NaI binned-group data.

[f]Present Ge(Li) data; values are averages obtained for one or more spectra having mean E_n within designated bin. Values in parentheses are similarly summed $d\sigma/d\omega$ for all discrete lines reported in the present experiment.

The lack of agreement for $E_\gamma < 2.4$ MeV is apparent in the unfolded results for $E_n > 5.1$ MeV. Errors in the response functions for low-energy gamma rays can be excluded as a major source of discrepancy in view of the fair agreement below $E_n = 5.1$ MeV. Our confidence in our low-energy gamma-ray response functions seems to be justified by the ^{226}Ra results shown in Figure 4. Some of the differences could come from an inadequate description of the low-energy Compton distribution of the response functions for high-energy gamma rays. It is not very easy to test directly the low-energy part of the response functions for high-energy gamma rays. Nevertheless, this possible source of disagreement does not appear to us to be capable of explaining completely the discrepancy. For our NaI detector, approximately 20% of the total response for 4.4 MeV gamma rays corresponds to a deposited energy between 0.7 and 2.4 MeV, and the response functions agree with that for an identical detector, with different shield, used at the ORNL Tower Shielding Facility.[22] The Tower Shielding Facility gamma-ray spectrometer response functions have been checked using thermal-capture measurements where high-energy gamma-ray transitions dominated the spectra. Furthermore, for $5.15 \leq E_n \leq 6.15$ MeV it is difficult to ascribe the 90 mb/sr difference between the GRT "Total" and our NaI "Total" to some error in the NaI response functions, for this would imply that more than 60% of the total response functions for high-energy gamma rays corresponded to a deposited energy between 0.7 and 2.4 MeV if $d\sigma(\text{"Partial"})/d\omega$ is 50 mb/sr as indicated for this E_n bin in Table 2. By the same reasoning we can probably eliminate, also from consideration as the sole source of the discrepancy, the inadequcies of the low-energy part of the response function of the GRT Ge(Li) detector.

We have compared very carefully the results of the unfolding of our data using the same neutron and gamma-ray energy intervals as the GRT data, and Figure 6 for $5.15 < E_n < 6.13$ MeV is typical of the results for all E_n intervals. Major discrepancies occur for $946 < E_\gamma < 1185$ keV and $1424 < E_\gamma < 1663$ keV where the NaI data show unmistakable deep minima, in addition the bin $1185 < E_\gamma < 1424$ keV has much higher values in the GRT data. These deep minima are very evident in our raw data shown in Figure 5. The LASL results[3] do reproduce the character of the present NaI results, in Figure 6, quite well. For the other E_n intervals, however, the LASL results are in much less agreement. The highest neutron energy group for which there is good overall agreement is $4.10 < E_n < 5.15$ MeV. In Table 3 we show the detailed comparison of the four sets of data for this neutron energy group. It can be seen that already for this neutron group the only systematic disagreement occurs for the gamma-ray bins from 946 to 1663 keV. On the basis of their line data and their unfolded spectrum, Orphan et al.[6] conclude that there is about 46 mb/sr of "continuum" for this energy group. On the basis of our Ge(Li) gamma-ray line data at 4.85 MeV, we conclude that there is no "continuum" contribution when we compare to our unfolded NaI data and about 20 mb/sr of "continuum" when we compare to the GRT Ge(Li) unfolded data, this "continuum" being entirely with gamma-ray energies from 946 to 1663 keV. However, for $5.15 < E_n < 6.15$ MeV the present results indicate a gamma-ray "continuum" of 35 mb/sr or 15% of the total we obtain, whereas the GRT data suggest about 130 mb/sr or 40% of their total results. This rather sudden increase of "continuum" suggested by the GRT results seems difficult to understand. Over half of the difference in the two sets of data again occurs for $946 < E_\gamma < 1663$ keV, with the GRT data being more

TABLE 3. COMPARISON OF SUMMED DISCRETE-LINE $d\sigma/d\omega$ AT E_n = 4.85±0.15 MeV WITH CONTINUUM (BINNED-GROUP) $d\sigma/d\omega$ FOR NEUTRON ENERGY INTERVAL 4.10 - 5.15 MeV[a]

Gamma-Ray Energy Interval (keV)	^{56}Fe Σ $d\sigma/d\omega$ (Elemental)		^{54}Fe (Elemental)	Summed Discrete Lines	Unfolding		Unfolding-Lines(ORNL)	
	Present Results	Orphan et al.	Present Results	Present	Ge(Li) Orphan, et al.	NaI Present	Ge(Li) Orphan,et.al.	NaI Present
708-946	89.8±4.8	87.9	0.6±0.1	90.4±4.9	91.2±7.1	91.7±1.7	+0.8±8.6	+1.3±5.2
946-1185	7.7±0.8	6.0	1.3±0.2	9.0±0.9	16.3±2.7	12.8±1.2	+7.3±2.8	+3.8±1.5
1185-1424	22.6±2.3	24.9	4.1±0.4	26.7±2.7	31.4±2.0	19.1±0.9	+4.7±3.4	-7.6±2.8
1424-1663	0.4±0.2		0.4±0.1	0.8±0.3	8.2±0.8	1.5±0.7	+7.4±0.8	+0.7±0.8
1663-1902	14.9±1.5	11.9	0.2±0.1	15.1±1.6	15.4±1.2	13.5±0.7	+0.3±2.0	-1.6±1.7
1902-2141	13.1±1.4	9.1	0.3±0.1	13.4±1.5	14.8±0.9	11.0±0.6	+1.4±1.7	-2.4±1.6
2141-2380	5.3±0.5	3.9		5.3±0.5	3.4±0.4	6.2±0.5	-1.5±0.6	+0.9±0.7
2380-2619	10.1±1.0	10.4	0.2±0.1	10.3±1.1	9.4±0.7	8.9±0.4	-0.9±1.3	-1.4±1.2
2619-2858	4.0±0.4	4.3	0.2±0.1	4.2±0.4	5.9±0.4	5.0±0.3	+1.7±0.6	+0.8±0.5
2858-3097	2.6±0.4		0.4±0.1	3.0±0.5	3.3±0.3	3.6±0.3	+0.3±0.6	+0.6±0.6
3097-3336	3.9±0.5	1.5	0.5±0.1	4.4±0.6	3.7±0.2	4.4±0.2	-0.7±0.4	+0.0±0.6
3336-3575	5.5±0.7	3.6		5.5±0.7	3.6±0.3	7.3±0.2	-1.9±0.8	+1.8±0.7
3575-3814	4.8±0.4	4.2		4.8±0.4	6.0±0.2	3.8±0.1	+1.2±0.4	-1.0±0.4
3814-4053	0.7±0.2			0.7±0.2	0.3±0.1	0.8±0.1	-0.4±0.2	+0.1±0.2
4053-4291					0.3±0.1	0.1±0.1	+0.3±0.1	+0.1±0.1
≥ 4291	0.4±0.2			0.4±0.2		0.3±0.2	-0.4±0.2	-0.1±0.3
Total				193.4±16.7	213.7±17.4	189.3±8.2		

[a]The gamma-ray energy intervals, neutron energy interval and data in colums 3 and 6 were reported in Gulf Radiation Technology Report RT-A10743 (see Ref. 6).

than twice as large as our data in those three gamma-ray bins. (Our NaI unfolded data give 50 mb/sr; their Ge(Li) unfolded data give 104 mb/sr.) According to our knowledge of the reaction mechanisms involved, it is difficult to understand this sudden jump in cross section between the two energy regions. In fact, for E_n between 4 and 12 MeV the total non-elastic cross sections are nearly constant at 1350-1400 mb,[7] i.e., $\sigma/4\pi$ = 110 mb/sr to use units comparable to Table 2. For E_n from 5 to 6 MeV, the differential cross sections for $^{56}Fe(n,\gamma)$, $^{56}Fe(n,p)$ and $^{56}Fe(n,\alpha)$ are all less than 1 mb/sr.[7] The $^{54}Fe(n,p)$ cross sections $\sigma/4\pi$ = 40 mb/sr[7] must be corrected for isotopic abundance of 5.8%, leaving about 2 mb/sr as the possible contribution from this reaction. Thus from 4 to 6 MeV incident neutron energy the dominant gamma-ray producing reaction is (n,n'). The only way to account for the sharp increase in the "Total" gamma-ray production data of GRT is to assume that there is a sharp increase in average gamma-ray multiplicity from 2 for $4.1 < E_n < 5.1$ MeV to 3 for $5.1 < E_n < 6.1$ MeV. To obtain such a large increase in average gamma-ray multiplicity implies a very large change in the multiplicity for the levels populated by 5- to 6-MeV neutrons as opposed to those populated by $\leq$ 5-MeV neutrons. Theoretical expectations[13] are that the average multiplicity increases by only 10% from 5 to 6 MeV. We emphasize that we do not disagree with the premise that some amount of "continuum" exists in the GRT measurements as well as our own; but we fail to understand the sudden jump at E_n = 5.1 MeV, particularly in view of the then almost constant value of the cross section up to 10 MeV.

The large decrease in the gamma-ray production cross section above 12 MeV, seen in our data, can be understood in terms of the onset of the (n,2n)

reaction. This reaction populates low-lying levels in the residual nucleus with small gamma-ray multiplicities at the expense of the (n,n') reaction, which populates the high excited states in the residual nucleus with much higher gamma-ray multiplicities. At 14.5 MeV, in the middle of the last neutron energy group of the GRT data, the (n,n') cross section with relatively high gamma-ray multiplicities is about equal to the sum of the (n,2n), (n,p) and (n,α) reactions which lead to much lower gamma-ray multiplicities. We, therefore, expect a reduction in the average multiplicity shown in our data but absent in the GRT data which gives the same value as in the interval $5 < E_n < 10$ MeV.

The above arguments suggest to us that the source of the discrepancies may be in the area where the two experiments differ most markedly - the determination of the background contribution for the unfolded spectra. For our experiment the assumptions underlying our background subtraction method have been detailed in Section II.

In the GRT experiment[6] the three main assumptions concerning the background subtraction from the iron data appear to be: 1) the background spectral shapes are determined by substituting a beryllium scatterer, using spectra obtained at incident neutron energies 1.344 times higher to compensate for the difference in kinematic energy loss for elastic scattering through 125°; 2) normalization for the background subtraction can be determined on the basis of the area of the 596-keV line from ^{74}Ge(n,n'γ); 3) the "background" and "foreground plus background" spectra can be unfolded first and then subtracted. We do not know how well these assumptions were verified for this experiment beyond what is stated in the report.[6] One may conjecture about

possible breakdowns in these assumptions on the basis of the information given in the report[6] which might explain the differences between their unfolded data and ours. We realize how conjectural the following remarks may be; we claim only that they appear to us plausible at the moment on the basis of the information in the report[6] and could possibly explain the areas of disagreement between the two sets of unfolded data. Up to a certain neutron energy, say E_n = 5 MeV, the procedure followed in using the beryllium data as background for the iron sample might be working well because of the similarity between the neutron energy spectra striking the detectors, i.e., mostly elastic scattering. Above this energy, say up to E_n = 12 MeV, the high-energy part of the background may also be obtained correctly because it is also dominated by the elastic scattering from both samples. However, the low-energy part of the background, say for $E_\gamma < 2.4$ MeV, comes from two sources: a) the high-energy elastically-scattered neutrons, and this would be obtained correctly and b) the low-energy neutrons, and this part of the background may not have been obtained correctly. This is because we suspect the (n,n') neutron spectrum from iron to be considerably harder than the (n,2n) neutron spectrum from beryllium; the "background", i.e., neutron induced counts in the Ge(Li) detector, might not have been subtracted enough in using the beryllium spectrum. Orphan et al.[6] do not claim to have used rigorously the areas in the 596-keV ^{74}Ge(n,n'γ) peaks to subtract the background from the data but to have also performed, at least at the lower energies, "any needed renormalization by matching the higher gamma-ray energy counts." It is, therefore, not obvious to us how any breakdown in this assumption, such as sensitivity of the 596-keV yield as a function of neutron energy spectra, might have affected the results. The above conjectures,

if correct, could possibly explain all of the similarity and differences in the two sets of data below 10 MeV. However, we do not have enough quantitative information to judge if the effects could be large enough to explain all of the observed differences. We do not think that the above arguments could account for much more than 2/3 of the differences above 10 MeV and, in particular, explain the discrepancy for $E_\gamma > 2.4$ MeV which is very large above 12.5 MeV. Orphan et al.[6] subtracted the "background" from the "foreground plus background" spectra after unfolding them. They state quite specifically that they prefer to do this rather than unfold the background corrected spectra because MAZE I, their unfolding code, "is sensitive to small inconsistencies in the spectrum being unfolded." If this is the case, we might think that the reverse procedure, unfolding the subtracted pulse-height spectrum, would be preferable in particular at high energies. The concept of unfolding a pulse-height spectrum is based on the premise that it can be decomposed by a superposition of lines having given response functions. If the pulse-height spectrum contains features, inconsistencies, which cannot be easily resolved with the response functions, it is not obvious how the unfolded spectrum is affected. At low energy, if the background is mostly coming from gamma rays induced in the germanium by the neutrons striking the detector, the procedure could be adequate provided the response functions used were also applicable to a gamma-ray source distributed inside the detector. But at high energies where in addition there is likely to be at least (n,p) and (n,α) reactions in the germanium, it is not clear to us what happens. In principle, if the background is subtracted from the pulse-height spectrum before unfolding, such that only counts from gamma rays for which the response functions have been obtained

remain in the spectrum, we have a much more reliable situation for the unfolding process.

IV. SUMMARY AND CONCLUSIONS

We have presented in this paper the results of our measurement of neutron-induced gamma-ray production cross sections for iron. The NaI detector system used at the ORELA Shield Test Station, the data acquisition and the reduction techniques employed were described in detail. Our Ge(Li) spectrometer data, acquired at the ORNL Van de Graaff, were briefly reported upon and used in comparisons with the NaI data. The bulk of the numerical values of the data was not given here as these are available in a separate report.[29]

Our data were compared in some detail with the results of an experiment, similar to our NaI measurement, performed at GRT[6] using a Ge(Li) spectrometer. The GRT data are of two types, line data and unfolded spectra. At 5 MeV the agreement between all four sets of data is very good, from 10% for strong lines to 20% for the weaker lines. The gamma-ray line data from the two Ge(Li) experiments are also within 10% for the strong lines in the region of overlap, $5 < E_n < 9$ MeV. (We have only shown the comparisons in a few instances, a more complete comparison being made in the GRT report.[6]) For the two strongest gamma-ray lines, at 846 and 1238 keV, we could make a comparison of our NaI data with the GRT line data and the agreement is of the order of 10% over the complete energy region. The agreement between the NaI and Ge(Li) unfolded data is not as good. More specifically, the data are in fair agreement up to $E_n = 5$ MeV, and for $5 < E_n < 10$ MeV we only find agreement for $E_\gamma > 2400$ keV. (For $5 < E_n < 10$ MeV

and for $950 < E_\gamma < 2400$ keV the data of GRT are approximately twice as large as ours.) Above $E_n = 10$ MeV, the disagreement increases for all gamma-ray energies, and in the region of $12.5 < E_n < 16.7$ MeV the overall disagreement is approximately a factor of two. We have investigated the nature of the disagreements in some detail, both from a point of view of the reaction mechanisms involved and the experimental techniques used in the two different experiments. We have indicated in two specific instances a few of the theoretical difficulties encountered in trying to understand some of the behavior of the GRT data. We conjecture that if the background contributions to the pulse-height spectra have been improperly subtracted in the GRT data, this could explain the discrepancies between the two sets of data.

V. ACKNOWLEDGEMENTS

We express our appreciation to W. E. Kinney, J. A. Biggerstaff, J. W. McConnell, P. H. Stelson, T. A. Love, H. A. Todd, S. Raman, and W. C. White for their contributions to this experimental program.

REFERENCES

1. Compilation of Requests for Nuclear Cross Section Measurements, Los Alamos Scientific Laboratory Report NCSAC-35 (March 1971); RENDA Compilation of EANDC Requests for Neutron Data Measurement, European Nuclear Energy Agency, O.E.C.D., Paris, Report No. EANDC 83 "U" (April 1970).

2. R. W. Benjamin, P. S. Buchanan and I. L. Morgan, Nucl. Phys. 79, 241 (1966).

3. D. M. Drake, J. C. Hopkins, C. S. Young and H. Conde, Nucl. Sci. Eng. 40, 294 (1970).

4. D. L. Broder, A. P. Gamaly, A. N. Lashchuk and Y. P. Sadokhin, Nuclear Data for Reactors, Proceedings of the Second International Conference on Nuclear Data for Reactors, Helsinski, June 1970, International Atomic Energy Agency (Vienna, 1970) p. 295.

5. G. Haouat, J. Lachkar, Y. Patin and J. Sigand, Proceedings of the Third Conference on Neutron Cross Sections and Technology, Knoxville, Tennessee, March 15-17, 1971, CONF-710301, Vol. 1, p. 202, U. S. Atomic Energy Commission, National Technical Information Service (1971).

6. V. J. Orphan, C. G. Hoot and Joseph John, Gulf Radiation Technology Report RT-A10743 (June 1971); V. J. Orphan, C. G. Hoot and Joseph John, Proceedings of the Third Conference on Neutron Cross Sections and Technology, Knoxville, Tennessee, March 15-17, 1971, CONF-710301, Vol. 1, p. 227, U. S. Atomic Energy Commission, National Technical Information Service (1971).

7. "Neutron Cross Sections," compiled by J. R. Stehn, M. D. Goldberg, B. A. Magurno and R. Wiener-Chasman, Brookhaven National Laboratory

Report No. BNL-325 (U. S. GPO., Washington, D. C. 1964), 2nd ed., Suppl. No. 2, Vol. 11-A.

8. M. E. Phelps, D. G. Sarantites and W. G. Winn, Nucl. Phys. A149, 647 (1970).

9. G. R. Meredith and D. C. Camp, Bull. Am. Phys. Soc. Ser. II 15, 478 (1970).

10. J. K. Dickens, Nucl. Sci. Eng. 48, 78 (1972).

11. G. L. Morgan, T. A. Love, J. K. Dickens and F. G. Perey, Gamma-Ray Production Cross Sections of Tantalum and Carbon for Incident Neutron Energies Between 0.007 and 20.0 MeV, ORNL-TM-3702 (February 1972).

12. E. Voss, S. Cierjacks and L. Kropp, Proceedings of the Third Conference on Neutron Cross Sections and Technology, Knoxville, Tennessee, March 15-17, 1971, CONF-710301, Vol. 1, p. 218, U. S. Atomic Energy Commission, National Technical Information Service (1971).

13. S. K. Penny and W. E. Kinney, A Re-Evaluation of Natural Iron Neutron and Gamma-Ray Production Cross Sections - ENDF/B Material 1124, ORNL-4617 (April 1971).

14. J. K. Dickens and F. G. Perey, Nucl. Sci. and Eng. 36, 280 (1969).

15. J. K. Dickens and F. G. Perey, Nucl. Sci. and Eng. 40, 283 (1970).

16. C. E. Burgart, E. A. Straker, T. A. Love and R. M. Freestone, Jr., Nucl. Sci. Eng. 42, 421 (1970).

17. V. V. Verbinski, W. R. Burrus, T. A. Love, W. Zobel and N. W. Hill, Nucl. Instr. Meth. 65, 8 (1968).

18. J. H. Todd, Instrumentation and Controls Div. Ann. Progr. Rept. Sept. 3, 1968, ORNL-4335, p. 17.

19. C. E. Burgart and R. M. Freestone, Jr., Neutron Phys. Div. Ann. Progr. Rept., May 31, 1971, ORNL-4705, p. 46.

20. H. E. Hall and T. W. Bonner, Nucl. Phys. 14, 295 (1959).

21. J. K. Dickens and F. G. Perey, Nucl. Sci. Eng. 40, 346 (1970).

22. J. K. Dickens and R. D. Baybarz, Nucl. Instr. Meth. 85, 143 (1970).

23. R. E. Maerker and F. J. Muckenthaler, Gamma-Ray Spectra from Thermal-Neutron Capture in Elements Found in Soils, Concrete, and Structural Materials, ORNL-4382 (June 1969).

24. J. K. Dickens, Energies and Intensities of Gamma Rays Emitted by a ^{226}Ra Source, ORNL-TM-3509 (August 1971).

25. R. Gunnink (Lawrence Radiation Laboratory), results communicated to ORNL Nuclear Data Group.

26. W. R. Burrus, Utilization of a priori Information by Means of Mathematical Programming in the Statistical Interpretation of Measured Distributions, ORNL-3743 (1965).

27. R. S. Booth, Nucl. Instr. Meth. 85, 69 (1970).

28. R. S. Booth and F. J. Muckenthaler, The Total Gamma-Ray Energy Spectrum Above 1 MeV from Neutron Interactions in ^{235}U and ^{238}U, ORNL-4691 (1971).

29. J. K. Dickens, G. L. Morgan and F. G. Perey, Gamma-Ray Production Due To Neutron Interactions with Iron For Incident Neutron Energies Between 0.8 and 20 MeV: Tabulated Differential Cross Sections, ORNL-4798 (July 1972).

30. J. K. Dickens and F. G. Perey, Nucl. Instr. and Meth. 82, 301 (1970).

31. J. K. Dickens, The ^{23}Na(n,xγ) Reaction for $4.85 \leq E_n \leq 7.5$ MeV, ORNL-TM-3737 (March 3, 1972); also to be published in Nucl. Sci. & Eng.

32. M. N. Rao, Nuclear Data B3, No. 3,4 P. 43ff (1970).

33. R. Gunnink, R. A. Meyer, J. B. Niday and R. P. Anderson, Nucl. Instr. Meth. 65, 26 (1968).

34. G. G. Seaman, N. Benczer-Koller, M. C. Bertin and Jack R. MacDonald, Phys. Rev. 188, 1706 (1969).

35. A. E. Blaugrund, Nucl. Phys. 88, 501 (1966).

36. H. Verheul, Nuclear Data B3, 5,6-161 (1970).

37. J. K. Dickens, "Level Structure of ^{54}Mn," ORNL-TM-3674 (January 14, 1972); also to be published in Phys. Rev.

38. F. G. Perey, W. E. Kinney and R. L. Macklin, Proceedings of the Third Conference on Neutron Cross Sections and Technology, Knoxville, Tennessee, March 15-17, 1971, CONF-710301, Vol. 1, p. 191, U. S. Atomic Energy Commission, National Technical Information Service (1971).

39. For comparison with the data in Ref. 6, the present results (e.g. Figure 5) were integrated between gamma-ray bin limits chosen to agree with Ref. 6. No physical significance is attached to the choices of bin limits.

40. L. Cranberg, A. H. Armstrong and R. L. Henkel, Phys. Rev. 104, 1639 (1956).

41. Preliminary reports of the present Ge(Li) results, J. K. Dickens and F. G. Perey, ORNL-4592, p. 32, were not corrected for this effect.

42. An earlier publication reports similar data using a NaI spectrometer; see D. L. Broder, A. G. Dovbenko, V. E. Kolesov, A. I. Lashchuk and I. P. Sadokhin, Izv. Akad. Nauk SSSR, Ser. Fiz. 31, 327 (1967); Trans. Bull. Academy of Sciences USSR, Phys. Ser. 31, 311 (1968) Columbia Technical Translations, White Plains, New York.

APPENDIX

TABULATED CROSS SECTIONS FOR NaI-SPECTROMETER DATA

NEUTRON GAMMA RAY PRODUCTION CROSS SECTIONS FROM IRON. THE TABULATED VALUES ARE DIFFERENTIAL CROSS SECTIONS AT 125 DEGREES, IN MB/SR, FOR THE GAMMA RAY ENERGY INTERVALS, IN KEV, SHOWN IN THE LEFTMOST COLUMN. THE ERRORS INDICATED ARE IN THE SAME UNITS AND DO NOT INCLUDE AN ESTIMATED 10% ERROR DUE TO THE ABSOLUTE FLUX MEASUREMENT. THE RELATIVE ERRORS FOR ADJACENT COLUMNS SHOULD BE LESS THAN 5%. THE COLUMN HEADINGS ARE, IN MEV, THE LOWER LIMIT OF THE NEUTRON ENERGY INTERVAL FOR THAT COLUMN. THE UPPER LIMIT FOR THE LAST NEUTRON ENERGY INTERVAL IS 5.003 MEV.

	0.800	1.011	1.500	2.008	2.505	3.009	3.516	4.009	4.494
707- 945	18.60 0.19	39.90 0.28	54.60 0.52	71.50 0.66	74.70 0.97	80.80 1.31	86.90 1.62	88.40 1.85	93.90 2.10
945-1184	0.20 0.03	0.40 0.05	1.85 0.12	1.34 0.19	2.90 0.39	3.53 0.70	6.80 1.03	10.60 1.25	13.90 1.47
1184-1423	0.02 0.03	0.17 0.03	1.42 0.08	3.76 0.14	7.83 0.30	10.90 0.56	13.40 0.80	16.60 0.99	19.90 1.11
1423-1662	0.02 0.02	0.10 0.02	1.13 0.05	1.16 0.07	1.35 0.17	1.19 0.25	1.10 0.44	0.95 0.23	1.72 0.85
1662-1901	0.01 0.00	0.01 0.02	0.06 0.02	0.20 0.04	4.42 0.16	10.90 0.42	10.90 0.59	12.30 0.74	14.20 0.84
1901-2140	0.02 0.03	0.02 0.02	0.01 0.00	0.07 0.04	0.40 0.07	7.59 0.33	9.26 0.55	10.60 0.69	11.10 0.81
2140-2379	0.02 0.01	0.01 0.01	0.03 0.02	0.05 0.03	0.27 0.06	4.69 0.21	6.91 0.47	6.12 0.60	6.40 0.71
2379-2618	0.02 0.02	-0.01 0.00	0.03 0.02	0.02 0.02	0.14 0.04	0.75 0.11	6.50 0.34	7.98 0.48	9.48 0.57
2618-2857	0.03 0.02	0.04 0.01	0.01 0.01	-0.01 0.01	0.06 0.03	0.33 0.08	2.96 0.22	4.71 0.35	5.03 0.44
2857-3096	0.01 0.02	0.02 0.01	0.02 0.01	0.00 0.00	-0.00 0.01	0.55 0.06	1.11 0.17	3.09 0.29	3.56 0.37
3096-3335	0.01 0.02	0.02 0.01	0.01 0.01	0.03 0.02	0.00 0.01	0.29 0.05	1.57 0.15	2.94 0.24	5.09 0.32
3335-3574	0.03 0.02	0.02 0.01	-0.02 0.01	0.01 0.00	-0.01 0.02	0.07 0.03	3.53 0.15	6.04 0.22	7.83 0.29
3574-3813	0.01 0.02	-0.00 0.01	0.02 0.01	-0.02 0.02	0.07 0.02	-0.02 0.03	1.11 0.08	2.51 0.13	4.33 0.18
3813-4052	0.03 0.02	-0.01 0.01	0.04 0.02	0.00 0.00	0.03 0.03	0.01 0.00	0.09 0.05	0.34 0.07	0.79 0.11
4052-4290	0.01 0.02	0.02 0.01	0.01 0.01	0.04 0.02	-0.01 0.02	0.07 0.03	0.01 0.04	0.03 0.05	0.10 0.08
4290-4529	-0.01 0.02	0.02 0.01	-0.01 0.01	-0.00 0.01	-0.01 0.02	0.00 0.00	0.03 0.04	-0.02 0.03	0.13 0.04
4529-4768	0.00 0.01	0.01 0.00	0.01 0.01	0.00 0.01	0.01 0.01	0.00 0.02	0.04 0.03	-0.02 0.04	0.18 0.05
4768-5007	0.03 0.02	-0.00 0.01	0.02 0.01	0.01 0.02	0.04 0.02	-0.01 0.02	-0.00 0.02	0.01 0.03	0.02 0.01
5007-5246	0.02 0.02	0.01 0.01	0.01 0.01	0.01 0.02	-0.02 0.01	0.01 0.01	0.03 0.02	0.03 0.03	0.02 0.02
5246-5485	0.01 0.02	0.04 0.01	-0.01 0.01	0.01 0.02	-0.00 0.00	0.01 0.02	0.05 0.03	0.01 0.02	-0.02 0.03
5485-5724	0.01 0.02	-0.00 0.00	0.01 0.01	0.00 0.01	0.02 0.01	0.04 0.02	0.01 0.02	-0.02 0.02	0.01 0.01
5724-5963	-0.00 0.00	-0.01 0.00	0.01 0.01	0.00 0.01	-0.01 0.01	-0.00 0.01	-0.01 0.02	0.01 0.02	0.05 0.02
5963-6202	0.02 0.02	0.03 0.01	0.01 0.01	0.03 0.01	0.01 0.00	-0.01 0.01	0.01 0.02	0.04 0.02	0.02 0.01
6202-6441	0.02 0.01	0.01 0.01	-0.01 0.01	0.00 0.01	0.03 0.01	-0.00 0.01	0.03 0.02	-0.03 0.03	-0.01 0.00
6441-6680	-0.01 0.01	-0.01 0.01	-0.01 0.00	-0.01 0.01	0.01 0.01	0.02 0.01	0.02 0.02	-0.00 0.01	0.00 0.01
6680-6919	-0.00 0.01	0.01 0.01	0.01 0.01	0.01 0.00	0.00 0.01	0.01 0.01	-0.01 0.01	0.04 0.02	0.01 0.01
6919-7158	0.01 0.01	0.02 0.01	0.02 0.01	0.02 0.01	0.00 0.01	-0.01 0.01	-0.02 0.01	0.01 0.01	-0.00 0.01
7158-7397	0.02 0.01	0.00 0.00	0.00 0.00	0.01 0.00	-0.00 0.00	0.00 0.01	0.01 0.01	0.00 0.01	-0.00 0.00
7397-7636	0.01 0.01	0.00 0.00	-0.01 0.01	-0.00 0.00	-0.00 0.00	0.03 0.01	0.01 0.01	0.01 0.01	0.01 0.01
7636-7875	0.01 0.01	0.01 0.01	0.00 0.00	0.01 0.01	0.01 0.01	0.01 0.01	0.01 0.01	0.01 0.01	0.02 0.01

NEUTRON GAMMA RAY PRODUCTION CROSS SECTIONS FROM IRON. THE TABULATED VALUES ARE DIFFERENTIAL CROSS SECTIONS AT 125 DEGREES, IN MB/SR, FOR THE GAMMA RAY ENERGY INTERVALS, IN KEV, SHOWN IN THE LEFTMOST COLUMN. THE ERRORS INDICATED ARE IN THE SAME UNITS AND DO NOT INCLUDE AN ESTIMATED 10% ERROR DUE TO THE ABSOLUTE FLUX MEASUREMENT. THE RELATIVE ERRORS FOR ADJACENT COLUMNS SHOULD BE LESS THAN 5%. THE COLUMN HEADINGS ARE, IN MEV, THE LOWER LIMIT OF THE NEUTRON ENERGY INTERVAL FOR THAT COLUMN. THE UPPER LIMIT FOR THE LAST NEUTRON ENERGY INTERVAL IS 9.463 MEV.

	5.003		5.524		6.038		6.523		7.012		7.495		8.029		8.468		9.028	
707- 945	97.30	3.26	94.90	3.63	92.00	3.91	90.50	3.94	89.10	4.06	85.50	4.07	82.30	4.71	80.50	4.48	77.10	4.81
945-1184	15.00	2.33	14.50	2.60	14.50	2.75	16.70	2.91	17.50	3.09	16.70	3.01	16.10	3.55	17.10	3.50	15.10	3.75
1184-1423	27.40	1.77	32.60	2.05	36.10	2.16	36.30	2.38	37.70	2.37	37.50	2.48	37.60	2.91	37.60	2.85	36.00	3.00
1423-1662	2.99	1.29	5.08	1.39	5.25	1.58	5.72	1.76	5.55	1.76	6.74	1.75	5.41	2.08	6.58	1.94	6.04	2.05
1662-1901	15.60	1.29	16.20	1.43	16.40	1.52	15.70	1.57	16.40	1.66	15.60	1.68	16.40	1.85	14.90	1.80	13.30	2.14
1901-2140	12.20	1.27	13.00	1.38	12.90	1.44	13.30	1.41	12.90	1.62	13.60	1.61	13.20	1.96	11.20	1.91	10.70	2.01
2140-2379	7.20	0.95	7.58	1.18	8.65	1.25	10.00	1.28	9.11	1.43	8.15	1.55	7.39	1.79	8.30	1.70	8.21	1.84
2379-2618	9.46	0.89	10.80	0.95	11.00	1.03	12.10	1.08	11.50	1.19	10.90	1.27	11.80	1.53	11.20	1.48	10.20	1.60
2618-2857	5.97	0.58	6.66	0.69	8.30	0.72	8.97	0.81	9.03	0.88	7.73	0.95	8.37	1.07	7.30	1.20	6.99	1.21
2857-3096	4.23	0.51	4.48	0.55	5.64	0.60	6.02	0.65	6.61	0.74	7.47	0.79	5.91	0.96	7.68	0.99	7.17	1.14
3096-3335	5.43	0.44	5.97	0.50	6.57	0.54	6.81	0.59	7.00	0.69	7.47	0.73	7.59	0.86	7.80	0.92	7.12	1.06
3335-3574	8.34	0.41	8.34	0.46	8.12	0.49	8.26	0.54	8.82	0.58	8.85	0.67	9.28	0.75	8.40	0.87	7.60	1.00
3574-3813	5.95	0.30	6.33	0.37	5.80	0.45	6.56	0.48	6.86	0.51	6.94	0.56	7.54	0.71	7.34	0.75	6.67	0.88
3813-4052	2.40	0.21	2.73	0.31	2.96	0.36	2.76	0.43	3.02	0.51	4.12	0.54	4.95	0.69	3.60	0.75	4.13	0.94
4052-4290	0.85	0.16	1.37	0.25	1.62	0.34	1.61	0.39	1.52	0.46	2.60	0.50	2.98	0.69	2.62	0.75	4.21	0.89
4290-4529	0.64	0.13	1.39	0.21	1.74	0.30	1.63	0.38	1.91	0.44	1.99	0.49	2.65	0.67	3.56	0.70	2.79	0.83
4529-4768	0.26	0.10	0.74	0.17	1.08	0.26	1.45	0.31	2.04	0.37	1.87	0.41	1.74	0.55	2.87	0.60	2.31	0.75
4768-5007	0.03	0.00	0.43	0.12	1.24	0.21	1.24	0.26	1.58	0.31	1.43	0.36	1.82	0.49	1.47	0.53	1.48	0.64
5007-5246	0.20	0.05	0.42	0.11	1.16	0.16	1.63	0.23	1.38	0.28	2.06	0.35	1.85	0.46	1.54	0.48	1.89	0.58
5246-5485	0.16	0.05	0.55	0.08	0.96	0.12	1.34	0.17	1.08	0.25	1.65	0.32	1.37	0.43	2.45	0.45	2.42	0.56
5485-5724	-0.01	0.01	0.25	0.06	0.43	0.10	0.78	0.15	1.18	0.22	1.23	0.31	1.24	0.42	1.86	0.43	1.70	0.55
5724-5963	0.00	0.03	0.03	0.05	0.17	0.08	0.44	0.12	1.58	0.20	1.20	0.30	1.11	0.40	0.94	0.44	1.58	0.55
5963-6202	-0.01	0.00	0.02	0.03	0.09	0.06	0.34	0.11	0.87	0.18	1.14	0.27	1.53	0.39	1.40	0.40	1.52	0.52
6202-6441	-0.00	0.02	0.02	0.03	-0.00	0.01	0.26	0.09	0.55	0.14	1.26	0.22	1.32	0.33	1.63	0.36	1.78	0.50
6441-6680	0.05	0.03	0.03	0.03	0.03	0.04	0.15	0.06	0.43	0.11	0.88	0.16	1.16	0.27	1.43	0.33	1.69	0.45
6680-6919	0.02	0.02	0.01	0.01	0.06	0.03	0.00	0.02	0.26	0.08	0.50	0.11	1.17	0.21	1.25	0.26	1.13	0.37
6919-7158	-0.00	0.01	-0.01	0.01	0.02	0.02	0.02	0.02	0.13	0.06	0.60	0.08	0.91	0.16	1.06	0.22	0.91	0.32
7158-7397	-0.02	0.02	0.01	0.01	-0.02	0.01	0.03	0.02	0.03	0.03	0.32	0.05	0.61	0.11	0.85	0.17	1.03	0.27
7397-7636	-0.01	0.01	0.01	0.01	-0.01	0.01	0.01	0.01	0.01	0.02	0.12	0.03	0.32	0.09	0.84	0.14	1.05	0.24
7636-7875	0.03	0.01	0.00	0.01	0.02	0.01	0.00	0.01	0.04	0.02	0.05	0.02	0.18	0.06	0.48	0.11	0.76	0.21

NEUTRON GAMMA RAY PPODUCTION CROSS SECTIONS FROM IRON.THE TABULATED VALUES ARE DIFFERENTIAL CROSS SECTIONS AT 125 DEGREES,IN MB/SR,FOR THE GAMMA RAY ENERGY INTERVALS,IN KEV,SHOWN IN THE LEFTMOST COLUMN.THE ERRORS INDICATED ARE IN THE SAME UNITS AND DO NOT INCLUDE AN ESTIMATED 10% ERROR DUE TO THE ABSOLUTE FLUX MEASUREMENT.THE RELATIVE ERRORS FOR ADJACENT COLUMNS SHOULD BE LESS THAN 5%.THE COLUMN HEADINGS ARE,IN MEV,THE LOWER LIMIT OF THE NEUTRON ENERGY INTERVAL FOR THAT COLUMN.THE UPPER LIMIT FOR THE LAST NEUTRON ENERGY INTERVAL IS 19.900 MEV.

	9.463		10.030		10.970		11.940		13.030		13.950		14.970		16.120		18.090	
707- 945	77.20	4.84	74.00	4.83	70.50	5.06	61.20	6.07	53.80	6.12	48.10	3.44	44.40	5.60	36.70	5.63	36.30	6.09
945-1184	15.10	3.72	14.90	3.57	15.00	3.96	14.70	4.28	13.20	4.64	14.20	4.39	14.20	4.18	10.70	3.75	13.80	4.59
1184-1423	40.20	2.98	40.70	2.87	42.40	3.13	41.00	3.65	36.30	3.90	31.10	3.93	27.30	3.56	27.50	3.23	27.90	3.86
1423-1662	6.12	2.12	6.74	1.97	5.22	2.24	7.25	2.37	7.01	2.51	5.82	2.37	6.58	2.26	6.09	2.03	6.69	2.52
1662-1901	12.50	1.96	12.50	2.05	12.80	2.08	10.60	2.41	9.47	2.50	8.54	2.21	5.38	2.36	5.32	1.89	7.48	2.31
1901-2140	10.00	1.92	9.55	2.02	10.10	2.02	8.19	2.35	6.34	2.60	6.37	2.44	4.09	2.39	3.16	1.82	3.22	2.70
2140-2379	6.88	1.84	6.97	1.87	6.14	2.01	6.72	2.20	6.18	2.28	3.48	2.06	1.48	0.62	4.89	1.68	4.27	2.33
2379-2618	10.40	1.50	9.19	1.59	10.00	1.72	9.03	1.79	7.34	2.30	4.82	1.97	3.35	1.24	2.77	1.51	4.08	1.81
2618-2857	8.69	1.27	7.43	1.18	6.62	1.37	6.38	1.60	5.77	1.53	3.92	1.54	3.82	1.53	1.56	1.18	3.01	1.42
2857-3096	7.51	1.11	6.85	1.01	6.35	1.18	6.17	1.34	3.46	1.35	4.37	1.44	5.23	1.23	3.86	1.02	1.44	1.41
3096-3335	7.57	1.09	7.54	0.95	7.74	1.08	7.52	1.25	5.47	1.42	3.95	1.31	1.32	1.14	2.85	0.95	4.69	1.22
3335-3574	6.45	1.05	8.32	0.90	7.41	1.08	5.37	1.20	4.83	1.21	2.61	1.35	2.96	1.24	2.43	0.90	4.36	1.14
3574-3813	6.22	0.93	6.71	0.87	6.89	1.09	5.75	1.14	5.57	1.29	3.35	1.27	2.96	1.16	2.07	0.91	2.82	1.16
3813-4052	4.34	0.97	4.47	0.93	4.39	1.10	4.72	1.25	4.26	1.36	3.51	1.28	1.97	1.24	0.46	0.96	0.63	0.31
4052-4290	3.86	0.87	3.83	0.94	2.82	1.15	4.94	1.28	2.39	1.47	1.86	1.34	1.11	1.27	1.78	0.91	0.49	1.07
4290-4529	2.81	0.86	3.14	0.85	3.27	1.06	1.41	1.29	3.25	1.39	2.13	1.29	0.84	1.22	0.74	0.91	1.04	1.01
4529-4768	2.09	0.74	2.30	0.78	3.86	0.90	1.56	1.03	1.95	1.14	2.22	1.15	1.81	1.01	1.89	0.82	2.04	0.84
4768-5007	2.78	0.64	3.14	0.65	2.74	0.81	3.52	0.91	1.58	1.06	2.15	1.00	1.51	0.91	1.35	0.68	0.70	0.80
5007-5246	2.62	0.62	2.67	0.63	3.03	0.71	3.03	0.84	3.42	0.98	1.33	0.92	1.72	0.88	0.11	0.07	0.29	0.41
5246-5485	3.03	0.58	2.58	0.57	3.12	0.71	1.88	0.83	2.33	1.00	1.58	0.92	0.81	0.77	0.32	0.62	0.10	0.14
5485-5724	2.01	0.58	2.60	0.57	1.38	0.74	2.57	0.87	1.62	0.95	1.37	0.93	-0.16	0.49	0.28	0.58	1.27	0.67
5724-5963	1.64	0.57	2.05	0.57	1.85	0.72	2.75	0.86	1.42	1.03	1.23	0.95	1.78	0.80	1.21	0.60	0.39	0.65
5963-6202	2.09	0.57	1.45	0.56	3.86	0.73	2.28	0.84	1.78	0.95	2.03	0.94	1.30	0.78	1.50	0.62	0.85	0.65
6202-6441	1.54	0.53	1.55	0.50	3.45	0.68	2.70	0.79	1.25	0.98	1.08	0.88	0.93	0.76	0.48	0.57	0.20	0.45
6441-6680	1.82	0.48	2.61	0.46	1.42	0.63	2.00	0.70	2.84	0.83	2.05	0.78	1.01	0.69	0.22	0.50	0.02	0.34
6680-6919	1.60	0.42	2.40	0.40	0.86	0.56	1.36	0.63	2.31	0.74	1.74	0.65	0.95	0.57	0.65	0.46	0.53	0.51
6919-7158	0.76	0.38	0.70	0.36	2.04	0.49	2.01	0.56	1.69	0.67	0.03	0.19	0.81	0.57	0.87	0.43	0.63	0.38
7158-7397	1.09	0.34	1.05	0.34	1.96	0.47	1.89	0.53	0.69	0.62	0.49	0.53	0.95	0.50	0.25	0.41	0.19	0.33
7397-7636	1.30	0.32	1.46	0.32	0.99	0.45	1.53	0.50	0.30	0.58	0.71	0.51	0.88	0.51	0.20	0.35	0.08	0.28
7636-7875	0.53	0.28	1.20	0.31	1.21	0.42	0.86	0.47	0.95	0.57	0.66	0.49	0.31	0.42	0.43	0.34	0.20	0.25

NEUTRON GAMMA RAY PRODUCTION CROSS SECTIONS FROM IRON.THE TABULATED VALUES ARE DIFFERENTIAL CROSS SECTIONS AT 125 DEGREES,IN MB/SR,FOR THE GAMMA RAY ENERGY INTERVALS,IN KEV,SHOWN IN THE LEFTMOST COLUMN.THE ERRORS INDICATED ARE IN THE SAME UNITS AND DO NOT INCLUDE AN ESTIMATED 10% ERROR DUE TO THE ABSOLUTE FLUX MEASUREMENT.THE RELATIVE ERRORS FOR ADJACENT COLUMNS SHOULD BE LESS THAN 5%.THE COLUMN HEADINGS ARE,IN MEV,THE LOWER LIMIT OF THE NEUTRON ENERGY INTERVAL FOR THAT COLUMN.THE UPPER LIMIT FOR THE LAST NEUTRON ENERGY INTERVAL IS 16.740 MEV.

	0.856		1.320		2.140		3.070		4.110		5.140		6.130		7.750		9.830		12.600	
707- 945	32.00	0.22	54.20	0.45	74.20	0.74	84.00	1.28	91.70	1.73	95.10	3.28	90.30	3.54	80.40	3.94	71.10	4.60	49.00	4.67
945-1184	0.21	0.03	1.45	0.10	2.20	0.27	5.43	0.76	12.80	1.22	14.40	2.36	16.40	2.65	16.30	3.03	14.80	3.45	13.60	3.42
1184-1423	0.02	0.01	1.20	0.06	6.25	0.20	12.30	0.59	19.10	0.92	31.00	1.78	36.80	2.07	37.60	2.42	41.40	2.74	32.50	2.86
1423-1662	0.02	0.02	0.84	0.04	1.30	0.11	1.13	0.44	1.51	0.71	4.20	1.27	5.91	1.50	5.89	1.70	6.14	1.92	6.59	1.73
1662-1901	0.01	0.02	0.06	0.02	2.56	0.09	10.90	0.44	13.50	0.68	16.30	1.25	16.00	1.40	14.90	1.54	11.90	1.84	8.40	1.73
1901-2140	0.02	0.02	0.02	0.02	0.44	0.05	8.66	0.37	11.00	0.64	12.70	1.22	13.30	1.27	11.80	1.54	9.58	1.72	5.70	1.80
2140-2379	0.01	0.02	0.02	0.02	0.22	0.04	6.08	0.28	6.19	0.55	7.51	0.97	9.19	1.12	7.67	1.42	6.85	1.63	4.32	1.53
2379-2618	0.00	0.00	0.02	0.02	0.08	0.03	3.67	0.18	8.87	0.44	10.20	0.82	11.40	0.91	11.10	1.16	9.45	1.35	5.54	1.39
2618-2857	0.03	0.01	0.01	0.01	0.04	0.02	1.74	0.12	5.01	0.32	6.39	0.55	8.72	0.64	7.56	0.84	7.57	1.03	4.19	1.03
2857-3096	0.01	0.01	0.02	0.01	0.01	0.02	0.90	0.09	3.59	0.26	4.42	0.46	6.25	0.51	7.18	0.72	6.71	0.87	4.29	0.86
3096-3335	0.02	0.01	0.03	0.01	0.01	0.02	0.94	0.07	4.41	0.22	5.73	0.41	7.05	0.46	7.41	0.66	7.36	0.80	4.61	0.79
3335-3574	0.02	0.01	0.00	0.00	-0.01	0.01	1.88	0.07	7.28	0.20	8.23	0.37	8.55	0.39	8.21	0.61	7.19	0.75	3.79	0.81
3574-3813	0.01	0.01	-0.01	0.01	0.03	0.02	0.60	0.05	3.78	0.12	6.18	0.28	6.43	0.34	7.06	0.47	6.72	0.72	3.85	0.73
3813-4052	0.01	0.01	0.03	0.01	0.00	0.00	0.07	0.03	0.76	0.08	2.66	0.21	3.04	0.29	4.28	0.48	4.53	0.74	3.02	0.78
4052-4290	0.01	0.02	0.02	0.01	0.02	0.02	0.04	0.03	0.12	0.05	1.18	0.17	1.68	0.25	3.24	0.44	3.71	0.74	2.29	0.81
4290-4529	0.01	0.01	-0.01	0.01	-0.00	0.01	0.00	0.00	0.06	0.03	1.22	0.14	1.82	0.24	2.73	0.43	2.80	0.69	2.24	0.80
4529-4768	0.01	0.01	0.00	0.01	0.02	0.01	0.01	0.01	0.13	0.04	0.57	0.11	1.61	0.20	2.02	0.36	2.73	0.59	1.74	0.62
4768-5007	0.01	0.01	0.02	0.01	0.01	0.01	-0.00	0.01	0.01	0.00	0.36	0.08	1.32	0.17	1.78	0.30	3.17	0.49	1.72	0.55
5007-5246	-0.00	0.01	0.02	0.01	-0.01	0.01	0.03	0.01	-0.01	0.02	0.40	0.07	1.51	0.14	1.99	0.27	2.75	0.45	2.16	0.52
5246-5485	0.03	0.01	-0.01	0.01	0.01	0.01	0.01	0.01	0.00	0.00	0.41	0.05	1.22	0.12	2.04	0.26	2.77	0.43	1.40	0.50
5485-5724	0.02	0.01	-0.01	0.01	0.02	0.01	0.01	0.01	0.01	0.01	0.12	0.05	0.80	0.11	1.60	0.24	2.25	0.44	1.27	0.51
5724-5963	-0.01	0.01	0.01	0.01	-0.00	0.00	-0.00	0.01	0.02	0.01	0.03	0.04	0.80	0.09	1.28	0.24	1.94	0.43	1.73	0.52
5963-6202	0.02	0.01	0.02	0.01	0.02	0.01	0.00	0.01	0.03	0.01	0.03	0.03	0.58	0.08	1.44	0.22	2.30	0.42	1.80	0.50
6202-6441	0.01	0.01	0.00	0.01	0.01	0.00	0.01	0.01	-0.02	0.01	0.01	0.02	0.37	0.07	1.47	0.20	2.36	0.38	1.29	0.50
6441-6680	-0.00	0.01	-0.01	0.01	-0.01	0.01	0.02	0.01	-0.00	0.00	0.03	0.02	0.25	0.05	1.33	0.17	2.17	0.35	1.86	0.42
6680-6919	0.01	0.01	0.01	0.00	0.00	0.00	0.00	0.01	0.03	0.01	0.01	0.01	0.14	0.04	1.17	0.14	1.67	0.30	1.58	0.36
6919-7158	0.01	0.01	0.02	0.01	0.02	0.01	-0.02	0.01	0.01	0.01	-0.02	0.01	0.12	0.03	0.95	0.11	1.25	0.27	1.01	0.33
7158-7397	0.01	0.01	0.01	0.00	0.01	0.01	0.01	0.01	-0.01	0.01	-0.01	0.01	0.04	0.01	0.77	0.09	1.46	0.25	0.94	0.30
7397-7636	0.01	0.01	-0.00	0.01	0.00	0.00	0.03	0.01	0.00	0.00	0.01	0.00	-0.01	0.01	0.62	0.08	1.39	0.24	0.80	0.29
7636-7875	0.01	0.01	0.01	0.00	0.00	0.00	0.00	0.01	0.02	0.00	0.02	0.01	0.01	0.01	0.38	0.07	1.06	0.22	0.65	0.27

INTERNAL DISTRIBUTION

1-3. L. S. Abbott
4. R. G. Alsmiller, Jr.
5. A. R. Buhl
6. C. E. Clifford
7-11. J. K. Dickens
12. C. Y. Fu
13. W. O. Harms
14. W. E. Kinney
15. T. A. Love
16. F. C. Maienschein
17-21. G. L. Morgan
22. F. J. Muckenthaler
23. F. R. Mynatt
24. E. M. Oblow
25. R. W. Peelle
26. S. K. Penny
27-41. F. G. Perey
42-51. R. W. Roussin (RSIC)
52. D. Sundberg
53. H. Feshbach (consultant)
54. H. Goldstein (consultant)
55. C. R. Mehl (consultant
56. H. T. Motz (consultant)
57-58. Central Research Library
59. ORNL Y-12 Technical Library
60. Document Reference Section
61-62. Laboratory Records
63. Laboratory Records ORNL RC
64. ORNL Patent Office
65-199. Laboratory Records (FREP)

EXTERNAL DISTRIBUTION

200. M. Drake, Brookhaven National Laboratory, Upton, L.I., New York 11973
201. Norman Francis, Knolls Atomic Power Laboratory, General Electric, Schenectady, New York 12309
202. Martin P. Fricke, Gulf Radiation Technology, P. O. Box 608, San Diego, California 92112
203. M. D. Goldberg, Brookhaven National Laboratory, Upton, L. I., New York 11973
204. H. Goldstein, Columbia University, 287A Eng. Terrace Bldg., 520 W. 120th St., New York, New York 10027
205. W. H. Hannum, Division of Reactor Development and Technology, AEC, Washington, D. C. 20546
206. P. B. Hemmig, Division of Reactor Development and Technology, AEC, Washington, D. C. 20546
207. C. E. Hollandsworth, USA Nuclear Effects Lab., Aberdeen Proving Ground, Maryland
208. J. C. Hopkins, Los Alamos Scientific Laboratory, Los Alamos, New Mexico 87544
209. R. L. Howerton, Lawrence Radiation Laboratory, Livermore, California 94550
210. Kermit Laughon, AEC Site Representative, ORNL
211. M. T. McEllistrem, University of Kentucky, Lexington, Kentucky 40506
212. Vic Orphan, Gulf Radiation Technology, P. O. Box 608, San Diego, California 92112
213. S. Pearlstein, Brookhaven National Laboratory, National Neutron Cross Section Center, Upton, L. I., New York 11973
214. A. B. Smith, Argonne National Laboratory, Argonne, Illinois 60440
215. Leona Stewart, Los Alamos Scientific Laboratory, Los Alamos, New Mexico 87544
216. J. A. Swartout, Union Carbide Corporation, New York, N. Y. 10017

217. W. E. Tucker, Texas Nuclear Corporation, 5805 Bullard Drive, Austin, Texas 78731
218. J. L. Weil, Physics Department, University of Kentucky, Lexington, Kentucky 40506
219. Research and Technical Support Division, AEC, ORO
220-221. Technical Information Center, Oak Ridge
222. Patent Office, AEC, ORO
223-352. DNA Radiation Transport Distribution